Nečas Center for Mathematical Modeling

Residual based error estimates for the space-time discontinuous Galerkin method applied to the compressible flows

V. Dolejší, F. Roskovec, M. Vlasák

Preprint no. 2015-06

http://ncmm.karlin.mff.cuni.cz/

Residual based error estimates for the space-time discontinuous Galerkin method applied to the compressible flows[☆]

Vít Dolejší[a,*], Filip Roskovec[a], Miloslav Vlasák[a]

[a] *Charles University Prague, Faculty of Mathematics and Physics, Sokolovská 83, 186 75 Praha, Czech Republic*

Abstract

We develop an adaptive numerical method for solution of the non-stationary compressible Navier-Stokes equations. This method is based on the space-time discontinuous Galerkin discretization, which employs high polynomial approximation degrees with respect to the space as well as to the time coordinates. We focus on the identification of the computational errors, following from the space and time discretizations and from the inexact solution of the arising nonlinear algebraic systems. We derive the residual-based error estimates approximating these errors. Then we propose an efficient algorithm which brings the algebraic, spatial and temporal errors under control. The computational performance of the proposed method is demonstrated by numerical experiments.

Keywords: space-time discontinuous Galerkin method, compressible Navier-Stokes equations, nonlinear algebraic problems, residual error estimates

1. Introduction

Our aim is to develop a sufficiently accurate and efficient numerical scheme for the simulation of unsteady viscous compressible flows. The *discontinuous Galerkin* (DG) method, based on a discontinuous piecewise polynomial approximation, is a popular technique for numerical solution of the compressible Navier-Stokes equations, we refer to the pioneering works [1, 2, 3, 4] and some recent papers [5, 6, 7, 8, 9, 10, 11, 12] and the references cited therein.

The space DG discretization leads to a system of stiff ordinary differential equations (ODEs) for which a suitable ODEs solver is needed. This approach has the advantage of permitting to use large time steps. In [13], we employed high order multistep *backward difference formulae* (BDF) for the time discretization. The BDF methods have lower computational costs in comparison to the implicit Runge-Kutta methods and the time discontinuous Galerkin discretization, since the size of the resulting nonlinear algebraic systems does not depend on the order of the BDF method. On the other hand, multistep methods are not suitable for computations using different meshes at different time levels, since re-computation of the solution from the triangulations corresponding to previous time levels to the actual one can cause a lost of accuracy. Therefore, we consider the *space-time discontinuous Galerkin* (STDG) method, which is more suitable for unsteady flow simulations.

The STDG method employs discontinuous piecewise polynomial approximation with respect to the space as well as to the time coordinates. On the other hand, the STDG method is very expensive, since the resulting algebraic systems are several times larger (depending on the polynomial approximation degree with respect to time) in comparison to the BDF methods. However, its computational costs are partly compensated by its higher accuracy with respect to

[☆]This work was supported by the Grant No. 13-00522S of the Czech Science Foundation and the membership in the Nečas Center for Mathematical Modeling (http://ncmm.karlin.mff.cuni.cz). The research of M. Vlasák was supported by the project MathMAC - University center for mathematical modeling, applied analysis and computational mathematics of the Charles University in Prague.

[*]Corresponding author (dolejsi@karlin.mff.cuni.cz)

time, allowing to use larger time steps, The STDG method for the compressible flow problems was developed in the series of papers by van der Vegt, van der Ven et al. ([15, 16, 17, 18, 19]), where the algebraic systems were solved by a pseudo-time stepping and h-multigrid techniques, and by et al. ([20, 21]) where the explicit local time stepping is employed. The analysis of the STDG method for a nonlinear convection-diffusion equation was presented in, e.g., [22, 23].

The numerical solution of the given system of nonlinear partial differential equations (PDEs) by the STDG method is influenced by three types of errors:

- *space* (or spatial) *error* resulting from the space semi-discretization of the given PDEs by the DG method,
- *time* (or temporal) *error* resulting from the discretization of the arising ODEs system with the aid of the time DG scheme,
- *algebraic error* (including rounding errors) resulting from the inexact solution of the corresponding nonlinear algebraic systems at each time step.

In order to ensure the accuracy as well as the efficiency of the numerical method, these errors should be balanced. Several theoretical papers deal with a posteriori error estimates for model nonlinear time-dependent problems, let us mention [24, 25, 26, 27, 28, 29] and the references therein. Concerning the compressible flow problem, a rigorous a posteriori numerical analysis is an open problem. There are only a few papers dealing with it, let us mention [30], which uses the so-called goal-oriented a posteriori error estimation for stationary compressible Navier-Stokes equations based on the approach [31], see also [32]. A similar idea was developed in [33, 34] for the space-time discontinuous Galerkin method applied to the Navier-Stokes equations.

Usually (see the papers cited above), the difference between the exact and the approximate solutions is estimated by an error estimator reflecting the space as well as the time discretizations. This estimator is often split into its spatial and temporal parts which reflect the space and time discretization separately (in some sense). In [13], we presented a different approach, where the spatial error is considered as a difference between the approximate (=space-time discrete) solution and the time semi-discrete solution (which is formally exact with respect to space). Similarly, the temporal error is considered as a difference between the approximate solution and the space semi-discrete solution (which is formally exact with respect to time). Thereafter, we derived (rather heuristic) residual error estimators which are able to identify the *space*, *time* and *algebraic errors*.

In this paper, we extend the approach from [13] to the STDG method. The aim is to develop an algorithm which leads to the numerical solution with the *smallest possible computational error* in the *shortest possible computational time* for the *given mesh*, the *given degree of polynomial approximation in space* and the *given degree of polynomial approximation in time*. Therefore, based on the mentioned residual error estimators, we define an algorithm which gives a numerical solution where the time and algebraic errors do not essentially contribute to the total computational error, the time partition is not too fine and the nonlinear algebraic systems are not over-solved. Moreover, we develop a mesh adaptation technique, which combines these residual error estimates with an *isotropic* and an *anisotropic* mesh refinement. The resulting scheme allows a local adaptation in space and a global adaptation in time during the computation. Finally, let us note that the presented approach is not limited to the application to the Navier-Stokes equations, it can be used for any time-dependent PDEs discretized by the STDG method.

The content of the rest of the paper is the following. In Section 2, we recall the system of the compressible Navier-Stokes equations and in Section 3 we introduce its discretization by the STDG method including the solution strategy of the arising nonlinear algebraic systems. Section 4 contains the main part of this paper, namely the derivation of the space, time and algebraic residual error estimators and the design of the final algorithm. The quantitative properties of these residual estimators are demonstrated in Section 5 for scalar convection-diffusion equations. Section 6 contains several numerical experiments demonstrating the applicability of the proposed algorithm to time-dependent inviscid and viscous compressible flows. Concluding remarks are presented in Section 7.

2. Compressible flow problem

Let $\Omega \subset \mathbb{R}^2$ be a polygonal domain and $T > 0$. We set $Q_T = \Omega \times (0,T)$ and by $\partial\Omega$, we denote the boundary of Ω which consists of several disjoint parts. We distinguish inlet, outlet and impermeable walls. The system of the Navier-Stokes equations describing the motion of a non-stationary viscous compressible flow can be written in the form

$$\frac{\partial \boldsymbol{w}}{\partial t} + \sum_{i=1}^{2} \frac{\partial \boldsymbol{f}_i(\boldsymbol{w})}{\partial x_i} = \sum_{i=1}^{2} \frac{\partial \boldsymbol{R}_i(\boldsymbol{w}, \nabla \boldsymbol{w})}{\partial x_i} \quad \text{in } Q_T, \tag{1}$$

where $\boldsymbol{w} = \boldsymbol{w}(x,t) : Q_T \to \mathbb{R}^4$, $\boldsymbol{w} = (\rho, \rho v_1, \rho v_2, e)^{\mathrm{T}}$ is the unknown state vector (ρ is the density, $\boldsymbol{v} = (v_1, v_2)$ is the vector of velocity and e is the energy), $\boldsymbol{f}_i : \mathbb{R}^4 \to \mathbb{R}^4$, $i = 1,2$ and $\boldsymbol{R}_i : \mathbb{R}^4 \times \mathbb{R}^8 \to \mathbb{R}^4$, $i = 1,2$, represents the inviscid and the viscous fluxes, respectively. The forms of vectors $\boldsymbol{f}_i$, $i = 1,2$, and $\boldsymbol{R}_i$, $i = 1,2$ can be found, e.g., in [35] or [36, Section 4.3].

We consider the Newtonian type of fluid accompanied by the state equation of a perfect gas and the definition of total energy. The system (1) is of *hyperbolic-parabolic* type and it is equipped with the initial condition $\boldsymbol{w}(x,0) = \boldsymbol{w}^0(x)$, $x \in \Omega$ and suitable boundary conditions. On the impermeable walls, we prescribe the no-slip condition and the adiabatic condition. On the inlet and outlet, we prescribe Dirichlet boundary conditions for some of the flow variables, while Neumann conditions are used for the remaining variables, see, e.g., in [35, 12, 36, 37, 13].

3. Space-time discontinuous Galerkin discretization

We briefly describe the discretization of (1) with the aid of the space-time discontinuous Galerkin (STDG) method. We use the standard notation for function spaces with usual norms and semi-norms (see, e. g., [38], [39]): $L^2(M)$ denotes the Lebesgue space of square integrable functions over a set M, $H^k(M)$, $k = 0,1,\dots$ are the Sobolev spaces of functions with square integrable weak derivatives of order k over M. The bolted symbols $\boldsymbol{H}^k(M)$, $k = 0,1,\dots$ denote Sobolev spaces of vector-valued functions from M to $\mathbb{R}^4$. By $(\cdot,\cdot)_\Omega$ we denote the L^2-scalar product over Ω.

Furthermore, $L^2(I;X)$ ($H^1(I;X)$) is the Bochner space of functions square integrable (square integrable first weak time derivative) over an interval $I \subset \mathbb{R}$ with values in a Banach space X.

3.1. Triangulations

Let $0 = t_0 < t_1 < \dots < t_r = T$ be a partition of $(0,T)$ generating time intervals $I_m = (t_{m-1}, t_m]$, $m = 1,\dots,r$ of the length $|I_m| = \tau_m$ and $\tau = \max_{m=1,\dots,r}\tau_m$. Obviously, the number of the time levels $r = r(\tau)$ depends on τ but we will not emphasize this dependence explicitly. Moreover, we set $\mathcal{I}_\tau := \{I_m\}_{m=1}^r$.

At every time level t_m, $m = 0,\dots,r$ we consider generally different space partition $\mathscr{T}_{h,m}$ consisting of a finite number of closed triangles K with mutually disjoint interiors and covering $\overline{\Omega}$, i.e., $\overline{\Omega} = \cup_{K\in\mathscr{T}_{h,m}} K$, $m = 0,\dots,r$. Moreover, we set $\mathscr{T}_h := \{\mathscr{T}_{h,m}\}_{m=1}^r$ and $h := \max_{m=1,\dots,r} \max_{K\in\mathscr{T}_{h,m}} \mathrm{diam}(K)$. The pair $\{\mathscr{T}_h, \mathcal{I}_\tau\}$ is called the *space-time* partition of the domain Q_T, see Figure 1 for a 1D illustration.

3.2. Functional spaces

Let $m = 0,\dots,r$ be arbitrary but fixed number denoting the index of the time slab. Let $\mathscr{T}_{h,m}$ be the triangulation, we define the so-called *broken Sobolev spaces*

$$H^2(\mathscr{T}_{h,m}) := \{v : \Omega \to \mathbb{R};\ v|_K \in H^2(K)\ \forall\, K \in \mathscr{T}_{h,m}\} \quad \text{and} \quad \boldsymbol{H}^2(\mathscr{T}_{h,m}) := [H^2(\mathscr{T}_{h,m})]^4$$

of scalar and vector-valued functions, respectively. Further, we define the *broken space-time space* over $\{\mathscr{T}_h, \mathcal{I}_\tau\}$ by

$$H^1(\mathcal{I}_\tau, \boldsymbol{H}^2(\mathscr{T}_h)) := \left\{\boldsymbol{\psi} : Q_T \to \mathbb{R}^4;\ \boldsymbol{\psi}|_{K\times I_m} \in H^1(I_m; \boldsymbol{H}^2(K)),\ K \in \mathscr{T}_{h,m},\ I_m \in \mathcal{I}_\tau,\ m = 1,\dots,r\right\}, \tag{2}$$

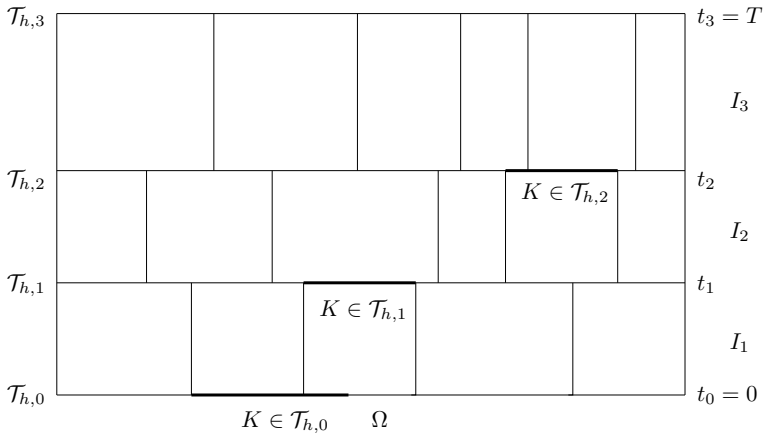

Figure 1: Space-time discretization of a one-dimensional domain Ω.

which consists of piecewise regular functions on space time elements $K \times I_m,\ K \in \mathscr{T}_{h,m},\ I_m \in \mathcal{I}_\tau$, which are in general discontinuous between two neighbouring elements $K, K' \in \mathscr{T}_{h,m}$ and between two time intervals $I_m, I_{m+1} \in \mathcal{I}_\tau$.

Moreover, we define the spaces of *discontinuous piecewise polynomial functions*. Although the discontinuous Galerkin method allows the use of different polynomial degrees over elements, we consider here the fixed degrees of polynomial approximation for all $K \in \mathscr{T}_{h,m},\ m = 0, \dots, r$, for simplicity.

First, we introduce the space of piecewise polynomial functions on the given mesh. Let $\mathscr{T}_{h,m}$ be a triangulation on the time level $I_m,\ m = 0, \dots, r$, we put

$$S_{m,h,p} = \{\varphi : \Omega \to \mathbb{R};\ \varphi(x)|_K \in P_p(K)\ \forall K \in \mathscr{T}_{h,m}\}, \quad \boldsymbol{S}_{m,h,p} := [S_{m,h,p}]^4, \tag{3}$$

where $P_p(K)$ denotes the space of all polynomials on K of degree $\le p$.

Furthermore, we define the spaces of functions on the space-time domain Q_T. Let $q \ge 0$ be an integer, we put

$$\boldsymbol{P}^q(\mathcal{I}_\tau) := \{\boldsymbol{v} : (0,T) \to \mathbb{R}^4,\ \boldsymbol{v}|_{I_m} \in [P^q(I_m)]^4,\ I_m \in \mathcal{I}_\tau\}, \tag{4}$$

where $P^q(I_m)$ is the space of polynomials of order $\le q$ on interval $I_m,\ m = 1, \dots, r$. Now, we define three subspaces of $H^1(\mathcal{I}_\tau, \boldsymbol{H}^2(\mathscr{T}_h))$, namely

$$H^1(\mathcal{I}_\tau; \boldsymbol{S}_{h,p}) := \left\{\boldsymbol{\psi} \in H^1(\mathcal{I}_\tau, \boldsymbol{H}^2(\mathscr{T}_h));\ \boldsymbol{\psi}(\cdot,t) \in \boldsymbol{S}_{m,h,p} \text{ for a.e. } t \in I_m,\ m = 1, \dots, r\right\}, \tag{5}$$

$$S^{\tau,q}(\mathcal{I}_\tau; \boldsymbol{H}^2(\mathscr{T}_h)) := \left\{\boldsymbol{\psi} \in H^1(\mathcal{I}_\tau, \boldsymbol{H}^2(\mathscr{T}_h));\ \boldsymbol{\psi}(x,\cdot) \in \boldsymbol{P}^q(\mathcal{I}_\tau) \text{ for a.e. } x \in \Omega\right\}, \tag{6}$$

$$S^{\tau,q}(\mathcal{I}_\tau; \boldsymbol{S}_{h,p}) := \left\{\boldsymbol{\psi} \in H^1(\mathcal{I}_\tau, \boldsymbol{H}^2(\mathscr{T}_h));\ \boldsymbol{\psi}|_{K\times I_m} \in [P^p(K) \times P^q(I_m)]^4, K \in \mathscr{T}_{h,m},\ I_m \in \mathcal{I}_\tau\right\}, \tag{7}$$

where $P^p(K) \times P^q(I_m)$ is the space of polynomials on $K \times I_m$ of the degree $\le p$ with respect to $x \in K$ and the degree $\le q$ with respect to $t \in I_m$ for $K \in \mathscr{T}_{h,m}$ and $I_m \in \mathcal{I}_\tau$. Therefore, all three spaces from (5)–(7) are piecewise regular on space time elements $K \times I_m,\ K \in \mathscr{T}_{h,m},\ I_m \in \mathcal{I}_\tau$, but generally discontinuous on Q_T. Moreover, $H^1(\mathcal{I}_\tau; \boldsymbol{S}_{h,p})$ consists of functions piecewise polynomial with respect to the space coordinates, $S^{\tau,q}(\mathcal{I}_\tau; \boldsymbol{H}^2(\mathscr{T}_h))$ consists of functions piecewise polynomial with respect to the time coordinate and $S^{\tau,q}(\mathcal{I}_\tau; \boldsymbol{S}_{h,p})$ consists of functions piecewise polynomial with respect to the space as well as the time coordinates.

Furthermore, we define the space of piecewise polynomial functions on each time slab

$$S^{\tau,q}(I_m; \boldsymbol{S}_{h,p}) := \left\{\boldsymbol{\psi} : \Omega \times I_m \to \mathbb{R}^4;\ \boldsymbol{\psi}|_{K\times I_m} \in [P^p(K) \times P^q(I_m)]^4, K \in \mathscr{T}_{h,m}\right\}. \tag{8}$$

Obviously, $\boldsymbol{\psi}|_{\Omega\times I_m} \in S^{\tau,q}(I_m; \boldsymbol{S}_{h,p})$ for all $\boldsymbol{\psi} \in S^{\tau,q}(\mathcal{I}_\tau; \boldsymbol{S}_{h,p}),\ m = 0, \dots, r$.

Finally, we introduce a jump of $\boldsymbol{\varphi} \in H^1(\mathcal{I}_\tau, \boldsymbol{H}^2(\mathscr{T}_h))$ with respect to time on the time level $t_m,\ m = 0, \ldots, r$ by

$$\{\!\{\boldsymbol{\varphi}\}\!\}_m := \boldsymbol{\varphi}|_m^+ - \boldsymbol{\varphi}|_m^-, \quad \boldsymbol{\varphi}|_m^\pm := \lim_{\delta \to 0\pm} \boldsymbol{\varphi}(t_m + \delta). \tag{9}$$

3.3. Space-time discontinuous Galerkin introduction

In order to proceed to the definition of the approximate solution, we carry out the *space semi-discretization* of the Navier-Stokes equations (1). We employ the incomplete interior penalty Galerkin (IIPG) discretization which was derived in details in [12, 13]. Therefore, we introduce here only the forms

$$\boldsymbol{a}_{h,m} : \boldsymbol{H}^2(\mathscr{T}_{h,m}) \times \boldsymbol{H}^2(\mathscr{T}_{h,m}) \to \mathbb{R}, \quad m = 1, \ldots, r \tag{10}$$

representing the DG discretization of inviscid and viscous fluxes of (1) on the mesh $\mathscr{T}_{h,m},\ m = 1, \ldots, r$. The form $\boldsymbol{a}_{h,m},\ m = 1, \ldots, r$ is linear with respect to its second argument and it is *consistent* with (1) in the following way: Let $\boldsymbol{w}$ be the regular solution of (1) with the corresponding initial and boundary condition then the following identity is valid

$$(\partial_t \boldsymbol{w}(t), \boldsymbol{\varphi})_\Omega + \boldsymbol{a}_{h,m}(\boldsymbol{w}(t), \boldsymbol{\varphi}) = 0 \qquad \forall \boldsymbol{\varphi} \in \boldsymbol{H}^2(\mathscr{T}_{h,m})\ \forall t \in I_m, \tag{11}$$

where we put $\partial_t := \partial/\partial t$.

Furthermore, using the standard DG discretization for parabolic problems (see, e.g., [40, Chapter 12] or [41]), we introduce the *space-time discontinuous Galerkin* (STDG) discretization of (1). For $m = 1, \ldots, r$, we define the forms

$$\boldsymbol{A}_{h,m}(\boldsymbol{w}, \boldsymbol{\psi}) := \int_{I_m} \{(\partial_t \boldsymbol{w}, \boldsymbol{\psi})_\Omega + \boldsymbol{a}_{h,m}(\boldsymbol{w}, \boldsymbol{\psi})\}\ \mathrm{d}t + \left(\{\!\{\boldsymbol{w}\}\!\}_{m-1}, \boldsymbol{\psi}|_{m-1}^+\right)_\Omega, \quad \boldsymbol{w}, \boldsymbol{\psi} \in H^1(\mathcal{I}_\tau, \boldsymbol{H}^2(\mathscr{T}_h)). \tag{12}$$

If $\boldsymbol{w}$ is the regular solution of (1) with the corresponding initial and boundary condition then, due to (11), we have

$$\boldsymbol{A}_{h,m}(\boldsymbol{w}, \boldsymbol{\psi}) = 0 \qquad \forall \boldsymbol{\psi} \in H^1(\mathcal{I}_\tau, \boldsymbol{H}^2(\mathscr{T}_h)). \tag{13}$$

The last term in (12)

$$\left(\{\!\{\boldsymbol{w}\}\!\}_{m-1}, \boldsymbol{\psi}|_{m-1}^+\right)_\Omega = \left(\boldsymbol{w}|_{m-1}^+, \boldsymbol{\psi}|_{m-1}^+\right)_\Omega - \left(\boldsymbol{w}|_{m-1}^-, \boldsymbol{\psi}|_{m-1}^+\right)_\Omega \tag{14}$$

couples the approximate solution from the consecutive time slaps, generally defined on different grids.

Now, we can introduce the space-time discontinuous Galerkin (STDG) discretization of (1).

Definition 3.1. *We say that the function* $\boldsymbol{w}_{h\tau} \in S^{\tau,q}(\mathcal{I}_\tau; \boldsymbol{S}_{h,p})$ *is the* space-time discrete solution *of problem* (1) *if*

$$\begin{aligned} &\boldsymbol{A}_{h,m}(\boldsymbol{w}_{h\tau}, \boldsymbol{\psi}) = 0 \quad \forall \boldsymbol{\psi} \in S^{\tau,q}(\mathcal{I}_\tau; \boldsymbol{S}_{h,p}),\ m = 1, \ldots, r, \\ &\left(\boldsymbol{w}_{h\tau}|_0^-, \boldsymbol{\varphi}\right)_\Omega = (\boldsymbol{w}_0, \boldsymbol{\varphi})_\Omega \quad \forall \boldsymbol{\varphi} \in S_{0,h,p}, \end{aligned} \tag{15}$$

where $\boldsymbol{w}_0$ *is the prescribed initial condition.*

Remark 3.2. *The relation* (15) *leads to nonlinear algebraic systems, which have to be solved* approximately *by an iterative method, cf. Section 3.4. The resulting solution is called the* approximate solution *which differs from the* space-time discrete solution *introduced above.*

The STDG method was analysed, e.g., in [22, 23] for the case of a scalar convection-diffusion equation. Based on those a priori error estimates and further numerical analysis (e.g. [42]) we expect that if the exact solution is from the Bochner space $H^{q+1}((0,T);H^s(\Omega)),\ s \geq 1$ then we have

$$\|e_{h\tau}\|_{L^2(0,T;H^1(\Omega))} \leq C_1 h^\mu + C_2 \tau^{q+1}, \quad \mu = \min(p, s-1), \tag{16}$$

where $\|e_{h\tau}\|_{L^2(0,T;H^1(\Omega))}$ is the discretization error in the broken $L^2(0,T;H^1(\Omega))$-seminorm, h is the size of the mesh step, τ is the size of the time step, p and q are the polynomial approximation degrees with respect to the space and the time coordinates, respectively, and $C_1 > 0$ and $C_2 > 0$ are constants independent of h and τ.

3.4. Solution strategy

The definition of the space-time discrete solution (15) represents a nonlinear algebraic system for each time level $m = 1, \dots, r$. Each system consists of $N_m = 2(p+1)(p+2)(q+1)\,\#\mathscr{T}_{h,m}$ equations, where $\#\mathscr{T}_{h,m}$ denotes the number of elements of $\mathscr{T}_{h,m}$ and p and q denote the polynomial approximation degree with respect to the space and the time coordinates, respectively. Using (15), we have to evaluate

$$\boldsymbol{w}_{h\tau}^m := \boldsymbol{w}_{h\tau}|_{\Omega \times I_m} \in S^{\tau,q}(I_m; \boldsymbol{S}_{h,p}) \qquad \text{for } m = 1, \dots, r. \tag{17}$$

The dimension $S^{\tau,q}(I_m; \boldsymbol{S}_{h,p})$ is equal to N_m.

Let $m = 1, \dots, r$ be arbitrary but fixed. By $B_{h,m} := \{\boldsymbol{\varphi}_i(x,t)\}_{i=1}^{N_m}$, we denote a set of linearly independent functions forming a basis of $S^{\tau,q}(I_m; \boldsymbol{S}_{h,p})$. It is possible to construct a basis $B_{h,m}$ as a composition of local bases constructed separately for each $K \times I_m,\ K \in \mathscr{T}_{h,m}$ and each component of the vector-valued functions.

Let $\boldsymbol{w}_{h\tau}^m \in S^{\tau,q}(I_m; \boldsymbol{S}_{h,p})$ be a piecewise polynomial function. It can be expressed as

$$\boldsymbol{w}_{h\tau}^m(x,t) = \sum_{j=1}^{N_m} \xi^{m,j} \boldsymbol{\varphi}_j(x,t) \in S^{\tau,q}(I_m; \boldsymbol{S}_{h,p}) \quad \longleftrightarrow \quad \boldsymbol{\xi}_m := \{\xi^{m,j}\}_{j=1}^{N_m} \in \mathbb{R}^{N_m}, \tag{18}$$

where $\xi^{m,j} \in \mathbb{R},\ j = 1, \dots, N_m,\ m = 1, \dots, r$ are the basis coefficients. Obviously, (18) defines an isomorphism between $S^{\tau,q}(I_m; \boldsymbol{S}_{h,p})$ and $\mathbb{R}^{N_m}$.

In order to rewrite the nonlinear algebraic systems (15), we define the vector-valued function $\boldsymbol{F}_{h,m} : \mathbb{R}^{N_m} \to \mathbb{R}^{N_m}$ by

$$\boldsymbol{F}_{h,m}(\boldsymbol{\xi}_m) := \{\boldsymbol{A}_{h,m}(\boldsymbol{w}_{h\tau}^m, \boldsymbol{\varphi}_i)\}_{i=1}^{N_m},\ m = 1, \dots, r. \tag{19}$$

We do not emphasize that $\boldsymbol{F}_{h,m}$ depends also on $\boldsymbol{w}_{h\tau}^{m-1}$. Therefore, the algebraic representation of the systems (15) reads:

$$\text{find } \boldsymbol{\xi}_m \in \mathbb{R}^{N_m} \text{ such that } \boldsymbol{F}_{h,m}(\boldsymbol{\xi}_m) = \boldsymbol{0}, \quad m = 1, \dots, r. \tag{20}$$

The system (20) is strongly nonlinear and we solve it by a Newton-like iterative method where the Jacobi matrix in the Newton method is replaced by the *flux matrix* developed in the context of the semi-implicit DG method in [35, 43, 12].

The forms $\boldsymbol{a}_{h,m},\ m = 1, \dots, r$ introduced in (10) satisfy

$$\boldsymbol{a}_{h,m}(\boldsymbol{w}, \boldsymbol{\varphi}) = \boldsymbol{a}_{h,m}^{\mathrm{L}}(\boldsymbol{w}, \boldsymbol{w}, \boldsymbol{\varphi}) - \boldsymbol{d}_{h,m}(\boldsymbol{w}, \boldsymbol{\varphi}) \qquad \forall \boldsymbol{w}, \boldsymbol{\varphi} \in \boldsymbol{H}^2(\mathscr{T}_{h,m})\ \forall t \in I_m, \tag{21}$$

where $\boldsymbol{a}_{h,m}^{\mathrm{L}}$ is a form, which is linear with respect to its second and third arguments and $\boldsymbol{d}_{h,m}$ is linear with respect to its second argument. The explicit relations of $\boldsymbol{a}_{h,m}^{\mathrm{L}}$ and $\boldsymbol{d}_{h,m}$ can be found in [13]. The form $\boldsymbol{a}_{h,m}^{\mathrm{L}}$ represents a linearization of $\boldsymbol{a}_{h,m}$.

Using (12) and (14), we define the $N_m \times N_m$ *flux matrix*

$$\mathbb{C}_{h,m}\left(\bar{\boldsymbol{\xi}}\right) := \left\{ \int_{I_m} \left\{ (\partial_t \boldsymbol{\varphi}_j, \boldsymbol{\varphi}_i)_\Omega + \boldsymbol{a}^{\mathrm{L}}_{h,m}(\bar{\boldsymbol{w}}, \boldsymbol{\varphi}_j, \boldsymbol{\varphi}_i) \right\} \, \mathrm{d}t + \left(\boldsymbol{\varphi}_j|^+_{m-1}, \boldsymbol{\varphi}_i|^+_{m-1}\right)_\Omega \right\}_{i,j=1}^{N_m} \tag{22}$$

and the vector

$$\boldsymbol{q}_{h,m}\left(\bar{\boldsymbol{\xi}}\right) := \left\{ \left(\bar{\boldsymbol{w}}|^-_{m-1}, \boldsymbol{\varphi}_i|^+_{m-1}\right)_\Omega + \boldsymbol{d}_{h,m}(\bar{\boldsymbol{w}}, \boldsymbol{\varphi}_i) \right\}_{i=1}^{N_m}, \tag{23}$$

where $\boldsymbol{\varphi}_i \in B_h,\ i = 1, \ldots, N_m$ are the basis functions, $\bar{\boldsymbol{\xi}} \in \mathbb{R}^{N_m}$ is the algebraic representation of $\bar{\boldsymbol{w}} \in S^{\tau,q}(I_m; \boldsymbol{S}_{h,p})$ given by (18). Finally, using (19) and (21) – (23), we have

$$\boldsymbol{F}_{h,m}(\boldsymbol{\xi}_m) = \mathbb{C}_{h,m}(\boldsymbol{\xi}_m)\boldsymbol{\xi}_m - \boldsymbol{q}_{h,m}(\boldsymbol{\xi}_m), \quad m = 1, \ldots, r. \tag{24}$$

Let us note that the flux matrix $\mathbb{C}_{h,m}$ has a block structure and it is sparse. Each block-row of $\mathbb{C}_{h,m}$ corresponds to one $K \in \mathscr{T}_{h,m}$ and it contains a diagonal block and several off-diagonal blocks. Each off-diagonal block corresponds to one neighbouring element of K. The sparsity of $\mathbb{C}_{h,m}$ is identical to the sparsity of the Jacobi matrix $D\boldsymbol{F}_{h,m}(\boldsymbol{\xi})/D\boldsymbol{\xi}$. Therefore, we use $\mathbb{C}_{h,m}$ as the approximation of $D\boldsymbol{F}_{h,m}(\boldsymbol{\xi})/D\boldsymbol{\xi}$ in the definition of our iterative Newton-like method. This approximation follows from relation (24), when we fix the arguments of $\mathbb{C}_{h,m}$ and $\boldsymbol{q}_{h,m}$ and perform the differentiation with respect to $\boldsymbol{\xi}_m$.

In order to determine solution $\boldsymbol{\xi}_m$ of the system (20), we employ a damped Newton-like method [44], which generates a sequence of approximations $\boldsymbol{\xi}^l_m$, $l = 0, 1, \ldots$ to the actual numerical solution $\boldsymbol{\xi}_m$ using the following algorithm. Given an iterate $\boldsymbol{\xi}^l_m$, the update $\boldsymbol{d}^l$ of $\boldsymbol{\xi}^l_m$ to get to the next iterate

$$\boldsymbol{\xi}^{l+1}_m := \boldsymbol{\xi}^l_m + \lambda^l \boldsymbol{d}^l \tag{25}$$

is defined by: find $\boldsymbol{d}^l \in \mathbb{R}^{N_m}$ such that

$$\mathbb{C}_{h,m}(\boldsymbol{\xi}^l_m)\boldsymbol{d}^l = -\boldsymbol{F}_{h,m}(\boldsymbol{\xi}^l_m), \tag{26}$$

where $\mathbb{C}_{h,m}$ is the flux matrix given by (22) and $\lambda^l \in (0, 1]$ is a damping parameter which enables convergence of (25) – (26) for larger class of problems, e.g., in case when the initial guess $\boldsymbol{\xi}^0_m$ is far from the solution of (20), cf. [44]. The numerical experiments presented in this paper were carried out with the following setting

- *Choice of the damping parameter.* We start from the value $\lambda^l = 1$ and evaluate a monitoring function $\delta^l := \left\| \boldsymbol{F}_{h,m}(\boldsymbol{\xi}^{l+1}_m) \right\| / \left\| \boldsymbol{F}_{h,m}(\boldsymbol{\xi}^l_m) \right\|$. If $\delta^l < 1$ we proceed to the next Newton iteration. Otherwise, we set $\lambda^l := \lambda^l/2$ and repeat the actual Newton iteration. Analysis of the convergence of the Newton method and the monitoring function can be found in [44].

- *Update of the flux matrix.* It is not necessary to update the flux matrix $\mathbb{C}_{h,m}(\boldsymbol{\xi}^l_m)$ at each Newton iteration $l = 1, 2, \ldots$ and each time level $m = 1, \ldots, r$. It is much cheaper to evaluate $\boldsymbol{F}_{h,m}$ than $\mathbb{C}_{h,m}$. Therefore, it is more efficient to perform more Newton iterations than to update $\mathbb{C}_{h,m}$. In practice, we update $\mathbb{C}_{h,m}$, either the damping parameter λ achieves a minimal prescribed value or the prescribed maximal number of Newton iteration was achieved.

- *Termination of the iterative process.* The iterative process (25) – (26) is terminated if a suitable *algebraic stopping criterion* is achieved. The standard approach is to set

$$\left\| \boldsymbol{F}_{h,m}(\boldsymbol{\xi}^l_m) \right\| \leq \eta, \tag{27}$$

  where $\|\cdot\|$ and η are a given norm and a given tolerance, respectively. However, it is difficult to choose TOL in order to guarantee the accuracy and in order to avoid an over-solution of the algebraic system. In Section 4.5, we present an *algebraic stopping criterion* following from the framework of residual error estimators.

- *Solution of the linear algebraic systems.* The linear algebraic systems (26) are solved by the GMRES method ([45]) with the block ILU(0) preconditioner, its sparsity is the same as the sparsity of matrix $\mathbb{C}$, see [12] for details. The solution from the previous Newton iteration is used as an initial condition for GMRES. In order not to oversolve the linear systems, we usually perform only few GMRES iterations, particularly we stop this iterative solver when the actual preconditioned residuum is ten times smaller than the initial one. This criterion may seem to be too weak, however, numerical experiments (not presented here) indicate that it is sufficient. A possible inaccuracy is controlled by the stopping criterion for nonlinear algebraic systems.

- *Choice of the time step.* We still have to specify the choice of the time steps $\tau_m,\ m = 1, \dots, r$ in (15). Obviously, too large time steps cause a decrease of accuracy and on the other hand, too small time steps lead to a decrease in efficiency. Standard approaches (e.g., [46], [47]) estimate the local discretization error of the time discretization of the ODE system. Then the choice of the size of the time step is based on this estimate in such a way that the local discretization error is under a given tolerance. However, this tolerance should be given (empirically) by a user. Our aim is to adapt the time step in such a way that the temporal error is controlled by the spatial one. In Section 4.5, we present an *adaptive choice of the time step* following from the framework of residual error estimators.

In the following, we denote by $\tilde{\boldsymbol{w}}_{h\tau} \in S^{\tau,q}(\mathcal{I}_\tau; \boldsymbol{S}_{h,p})$ the function corresponding to the output of the Newton-like iterative algorithm (25) – (26), i.e.,

$$\tilde{\boldsymbol{w}}_{h\tau}|_{I_m} := \tilde{\boldsymbol{w}}_{h\tau}^m \in S^{\tau,q}(I_m; \boldsymbol{S}_{h,p}), \qquad m = 1, \dots, r, \tag{28}$$

where $\tilde{\boldsymbol{w}}_{h\tau}^m$ is the piece-wise polynomial function corresponding to $\boldsymbol{\xi}_m^l$ by the isomorphism (18); l is the minimal index satisfying the stopping criterion. We call $\tilde{\boldsymbol{w}}_{h\tau}$ the *approximate solution* of problem (1). Obviously, due to inexact solution of (20), the approximate solution $\tilde{\boldsymbol{w}}_{h\tau}$ violates relation (15), cf. Remark 3.2.

4. Error estimates

In this section we present the main novelty of this paper. We have defined the STDG solution of the Navier-Stokes equations by (15), which was solved with the aid of the iterative algorithm (25) – (26). The total computational error (= the difference between the (unknown) exact solution and approximate solution resulting from (25) – (26)) depends on the following discretization parameters:

- space meshes $\mathscr{T}_h$ and the degree of polynomial approximation p with respect to the space coordinates,

- time partition $\mathcal{I}_\tau$ and the degree of polynomial approximation q with respect to the time coordinate,

- an inexactness of the iterative solver represented by the violation of $\boldsymbol{F}_{h,m}(\boldsymbol{\xi}_m) = \boldsymbol{0}$ introduced in (20).

Our goal is to identify the errors originating from the space discretization, from the time discretization and algebraic errors resulting from the inaccurate solution of (20). Particularly, we want to determine a stopping criterion for the iterative algorithm (25) – (26) and the strategy for adaptive choice of the time step in such a way that

- the resulting approximate STDG solution is not essentially influenced by the time discretization and algebraic errors,

- the time partition $\mathcal{I}_\tau$ is not too fine and the nonlinear algebraic systems are not over-solved.

4.1. Space, time, space-time and approximate solutions

We slightly reformulate the STDG discretization and introduce the *space semi-discrete* and the *time semi-discrete* solutions using the functional spaces (5) – (7). We define the form $\boldsymbol{A}_{h\tau}(\boldsymbol{z},\boldsymbol{\psi}) : H^1(\mathcal{I}_\tau,\boldsymbol{H}^2(\mathscr{T}_h)) \times H^1(\mathcal{I}_\tau,\boldsymbol{H}^2(\mathscr{T}_h)) \to \mathbb{R}$ by

$$\boldsymbol{A}_{h\tau}(\boldsymbol{z},\boldsymbol{\psi}) := \sum_{m=1}^{r} \boldsymbol{A}_{h,m}(\boldsymbol{z},\boldsymbol{\psi}), \qquad \boldsymbol{z},\boldsymbol{\psi} \in H^1(\mathcal{I}_\tau,\boldsymbol{H}^2(\mathscr{T}_h)). \tag{29}$$

where $\boldsymbol{A}_{h,m},\ m = 1,\dots,r$ are given by (12) and the space $H^1(\mathcal{I}_\tau,\boldsymbol{H}^2(\mathscr{T}_h))$ is defined by (2).

Let $\boldsymbol{w} \in H^1(0,T,\boldsymbol{H}^2(\Omega))$ formally denote the exact solution of the Navier-Stokes equations (1) satisfying the corresponding initial and boundary conditions. The consistency (13) implies that the *exact solution* $\boldsymbol{w}$ satisfies the identity

$$\boldsymbol{A}_{h\tau}(\boldsymbol{w},\boldsymbol{\psi}) = 0 \qquad \forall \boldsymbol{\psi} \in H^1(\mathcal{I}_\tau,\boldsymbol{H}^2(\mathscr{T}_h)). \tag{30}$$

Moreover, let $\boldsymbol{w}_{h\tau} \in S^{\tau,q}(\mathcal{I}_\tau;\boldsymbol{S}_{h,p})$ be the *space-time discrete solution* given by (15). Then (29) implies

$$\boldsymbol{A}_{h\tau}(\boldsymbol{w}_{h\tau},\boldsymbol{\varphi}_{h\tau}) = 0 \quad \forall \boldsymbol{\varphi}_{h\tau} \in S^{\tau,q}(\mathcal{I}_\tau;\boldsymbol{S}_{h,p}). \tag{31}$$

Furthermore, we define the *time semi-discrete* solution of (1) with the aid of the consistency identity (11) which formally represents an infinitely dimensional system of ODEs. Applying the time discontinuous Galerkin discretization to (11), we obtain the following problem: We seek $\boldsymbol{w}_\tau \in S^{\tau,q}(\mathcal{I}_\tau;\boldsymbol{H}^2(\mathscr{T}_h))$ such that

$$\begin{aligned} &\boldsymbol{A}_{h,m}(\boldsymbol{w}_\tau,\boldsymbol{\psi}) = 0 \quad \forall \boldsymbol{\psi} \in S^{\tau,q}(\mathcal{I}_\tau;\boldsymbol{H}^2(\mathscr{T}_h)),\ m = 1,\dots,r, \\ &\big(\boldsymbol{w}_\tau|_0^-,\boldsymbol{\varphi}\big)_\Omega = (\boldsymbol{w}_0,\boldsymbol{\varphi})_\Omega \quad \forall \boldsymbol{\varphi} \in \boldsymbol{H}^2(\mathscr{T}_{h,0}), \end{aligned} \tag{32}$$

where $\boldsymbol{w}_0$ is the prescribed initial condition. This together with (29) gives

$$\boldsymbol{A}_{h\tau}(\boldsymbol{w}_\tau,\boldsymbol{\psi}) = 0 \quad \forall \boldsymbol{\psi} \in S^{\tau,q}(\mathcal{I}_\tau;\boldsymbol{H}^2(\mathscr{T}_h)). \tag{33}$$

Finally, using (11), we define the *space semi-discrete* solution of (1): Find $\boldsymbol{w}_h \in H^1(\mathcal{I}_\tau;\boldsymbol{S}_{h,p})$ such that

$$\begin{aligned} &(\partial_t \boldsymbol{w}_h(t),\boldsymbol{\varphi})_\Omega + \boldsymbol{a}_{h,m}(\boldsymbol{w}_h(t),\boldsymbol{\varphi}) = 0 \qquad \forall \boldsymbol{\varphi} \in H^1(I_m,\boldsymbol{S}_{m,h,p})\ \forall t \in I_m,\ m = 1,\dots,r, \\ &\big(\boldsymbol{w}_h|_{m-1}^+,\boldsymbol{\varphi}\big)_\Omega = \big(\boldsymbol{w}_h|_{m-1}^-,\boldsymbol{\varphi}\big)_\Omega \quad \forall \boldsymbol{\varphi} \in \boldsymbol{S}_{m,h,p}. \end{aligned} \tag{34}$$

This together with (29) gives

$$\boldsymbol{A}_{h\tau}(\boldsymbol{w}_h,\boldsymbol{\psi}) = 0 \quad \forall \boldsymbol{\psi} \in H^1(\mathcal{I}_\tau;\boldsymbol{S}_{h,p}). \tag{35}$$

We summarise the "solutions" of the Navier-Stokes equations (1) introduced above:

- *exact solution* $\boldsymbol{w} \in H^1(0,T;\boldsymbol{H}^2(\Omega)) \subset H^1(\mathcal{I}_\tau,\boldsymbol{H}^2(\mathscr{T}_h))$ satisfying (30),
- *space semi-discrete solution* $\boldsymbol{w}_h \in H^1(\mathcal{I}_\tau;\boldsymbol{S}_{h,p})$ satisfying (35),
- *time semi-discrete solution* $\boldsymbol{w}_\tau \in S^{\tau,q}(\mathcal{I}_\tau;\boldsymbol{H}^2(\mathscr{T}_h))$ satisfying (33),
- *space-time discrete solution* $\boldsymbol{w}_{h\tau} \in S^{\tau,q}(\mathcal{I}_\tau;\boldsymbol{S}_{h,p})$ satisfying (31),
- *approximate solution* $\tilde{\boldsymbol{w}}_{h\tau} \in S^{\tau,q}(\mathcal{I}_\tau;\boldsymbol{S}_{h,p})$ given by (28), which violates (31) due to an inaccurate solution of the corresponding algebraic systems.

The relations among them are viewed in Figure 2.

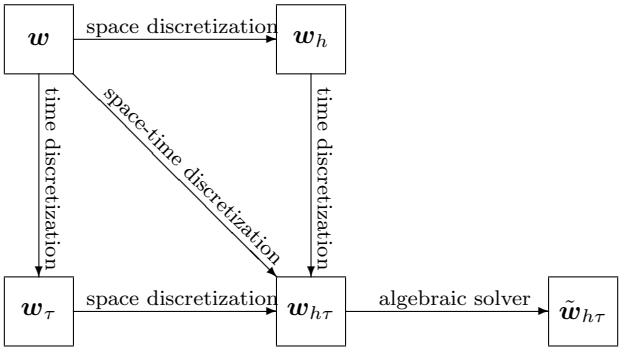

Figure 2: Types of the solutions and the errors

4.2. Error measures and error estimators

Similarly as in, e.g., [48, 49, 50, 29], we employ an error measure in the dual norm in the following way. Let V be a linear vector space with a norm $\|\cdot\|_V$, (the space V does not need to be complete with respect to $\|\cdot\|_V$) and let $a(\cdot,\cdot) : V \times V \to \mathbb{R}$ be a form linear with respect to its second argument and let V_h be a finite dimensional subspace of V. Moreover, let $u \in V$ and $u_h \in V_h$ be an exact and approximate solution of a fictitious problem defined by

$$a(u,\varphi) = 0 \quad \forall \varphi \in V \qquad \text{and} \qquad a(u_h,\varphi_h) = 0 \quad \forall \varphi_h \in V_h, \tag{36}$$

respectively. Then the *error measure in the dual norm* on the space V is given by

$$E(u_h) := \|Au_h - Au\|_{V'} := \sup_{\substack{\varphi\in V\\ \varphi\neq 0}} \frac{a(u_h,\varphi) - a(u,\varphi)}{\|\varphi\|_V} = \sup_{\substack{\varphi\in V\\ \varphi\neq 0}} \frac{a(u_h,\varphi)}{\|\varphi\|_V}, \tag{37}$$

where A is the operator from V to its dual space corresponding to $a(\cdot,\cdot)$ given by $\langle Au,\varphi\rangle := a(u,\varphi),\ u,\varphi \in V$, where $\langle\cdot,\cdot\rangle$ denotes the duality between V and V'. The last equality in (37) follows from (36). The equivalence between the error and the residual was analysed in [27, 28].

In Section 4.1, we introduced 5 types of the solution, which are drawn in Figure 2. Obviously, only the approximate solution $\tilde{\boldsymbol{w}}_{h\tau}$ is practically available. Moreover, taking into account the relations from Figure 2, we observe that

- the difference $\boldsymbol{w} - \tilde{\boldsymbol{w}}_{h\tau}$ represents the total computational error, i.e., the space and time discretization error and the inexactness of the algebraic solver,
- the difference $\boldsymbol{w}_h - \tilde{\boldsymbol{w}}_{h\tau}$ represents the time discretization error and the inexactness of the algebraic solver,
- the difference $\boldsymbol{w}_\tau - \tilde{\boldsymbol{w}}_{h\tau}$ represents the space discretization error and the inexactness of the algebraic solver,
- the difference $\boldsymbol{w}_{h\tau} - \tilde{\boldsymbol{w}}_{h\tau}$ represents the inexactness of the algebraic solver.

Based on these observations and in virtue of (36) – (37), we introduce an error measure of the approximate solution, particularly the *space-time* (total) *error*, the *time error*, the *space error* and the (nonlinear) *algebraic error*.

Space-time error is defined as the difference between the exact solution $\boldsymbol{w}$ and the approximate solution $t\boldsymbol{w}_{h\tau}$ in the dual norm of the space $H^1(\mathcal{I}_\tau, \boldsymbol{H}^2(\mathscr{T}_h))$, namely

$$\mathscr{E}_{\mathrm{ST}}(\tilde{\boldsymbol{w}}_{h\tau}) := \sup_{\substack{\boldsymbol{\psi}\in H^1(\mathcal{I}_\tau,\boldsymbol{H}^2(\mathscr{T}_h))\\ \boldsymbol{\psi}\neq 0}} \frac{\boldsymbol{A}_{h\tau}(\tilde{\boldsymbol{w}}_{h\tau},\boldsymbol{\psi}) - \boldsymbol{A}_{h\tau}(\boldsymbol{w},\boldsymbol{\psi})}{\|\boldsymbol{\psi}\|_X} = \sup_{\substack{\boldsymbol{\psi}\in H^1(\mathcal{I}_\tau,\boldsymbol{H}^2(\mathscr{T}_h))\\ \boldsymbol{\psi}\neq 0}} \frac{\boldsymbol{A}_{h\tau}(\tilde{\boldsymbol{w}}_{h\tau},\boldsymbol{\psi})}{\|\boldsymbol{\psi}\|_X}, \tag{38}$$

where $\|\cdot\|_X$ is a norm defined on $H^1(\mathcal{I}_\tau, \boldsymbol{H}^2(\mathscr{T}_h))$ (and on all its subspaces of course) and it will be specified later. The equality in (38) follows from (30).

Time error is defined as the difference between the space semi-discrete solution $\boldsymbol{w}_h$ (which is formally exact in time) and the approximate solution $\tilde{\boldsymbol{w}}_{h\tau}$ in the dual norm of the space $H^1(\mathcal{I}_\tau; \boldsymbol{S}_{h,p})$, namely

$$\mathscr{E}_{\mathrm{T}}(\tilde{\boldsymbol{w}}_{h\tau}) := \sup_{\substack{\boldsymbol{\psi}\in H^1(\mathcal{I}_\tau;\boldsymbol{S}_{h,p})\\ \boldsymbol{\psi}\neq 0}} \frac{\boldsymbol{A}_{h\tau}(\tilde{\boldsymbol{w}}_{h\tau},\boldsymbol{\psi}) - \boldsymbol{A}_{h\tau}(\boldsymbol{w}_h,\boldsymbol{\psi})}{\|\boldsymbol{\psi}\|_X} = \sup_{\substack{\boldsymbol{\psi}\in H^1(\mathcal{I}_\tau;\boldsymbol{S}_{h,p})\\ \boldsymbol{\psi}\neq 0}} \frac{\boldsymbol{A}_{h\tau}(\tilde{\boldsymbol{w}}_{h\tau},\boldsymbol{\psi})}{\|\boldsymbol{\psi}\|_X}, \tag{39}$$

where the equality follows from (35).

Space error is defined as the difference between the time semi-discrete solution $\boldsymbol{w}_\tau$ (which is formally exact in space) and the approximate solution $\tilde{\boldsymbol{w}}_{h\tau}$ in the dual norm of the space $S^{\tau,q}(\mathcal{I}_\tau; \boldsymbol{H}^2(\mathscr{T}_h))$, namely

$$\mathscr{E}_{\mathrm{S}}(\tilde{\boldsymbol{w}}_{h\tau}) := \sup_{\substack{\boldsymbol{\psi}\in S^{\tau,q}(\mathcal{I}_\tau;\boldsymbol{H}^2(\mathscr{T}_h))\\ \boldsymbol{\psi}\neq 0}} \frac{\boldsymbol{A}_{h\tau}(\tilde{\boldsymbol{w}}_{h\tau},\boldsymbol{\psi}) - \boldsymbol{A}_{h\tau}(\boldsymbol{w}_\tau,\boldsymbol{\psi})}{\|\boldsymbol{\psi}\|_X} = \sup_{\substack{\boldsymbol{\psi}\in S^{\tau,q}(\mathcal{I}_\tau;\boldsymbol{H}^2(\mathscr{T}_h))\\ \boldsymbol{\psi}\neq 0}} \frac{\boldsymbol{A}_{h\tau}(\tilde{\boldsymbol{w}}_{h\tau},\boldsymbol{\psi})}{\|\boldsymbol{\psi}\|_X}, \tag{40}$$

where the equality follows from (33).

Algebraic error is defined as the difference between the space-time discrete solution $\boldsymbol{w}_{h\tau}$ (which formally represents the approximate solution obtained by an exact algebraic solver) and the approximate solution $\tilde{\boldsymbol{w}}_{h\tau}$ in the dual norm of the space $S^{\tau,q}(\mathcal{I}_\tau; \boldsymbol{S}_{h,p})$, namely

$$\mathscr{E}_{\mathrm{A}}(\tilde{\boldsymbol{w}}_{h\tau}) := \sup_{\substack{\boldsymbol{\psi}_h\in S^{\tau,q}(\mathcal{I}_\tau;\boldsymbol{S}_{h,p})\\ \boldsymbol{\psi}_h\neq 0}} \frac{\boldsymbol{A}_{h\tau}(\tilde{\boldsymbol{w}}_{h\tau},\boldsymbol{\psi}_h) - \boldsymbol{A}_{h\tau}(\boldsymbol{w}_{h\tau},\boldsymbol{\psi}_h)}{\|\boldsymbol{\psi}_h\|_X} = \sup_{\substack{\boldsymbol{\psi}_h\in S^{\tau,q}(\mathcal{I}_\tau;\boldsymbol{S}_{h,p})\\ \boldsymbol{\psi}_h\neq 0}} \frac{\boldsymbol{A}_{h\tau}(\tilde{\boldsymbol{w}}_{h\tau},\boldsymbol{\psi}_h)}{\|\boldsymbol{\psi}_h\|_X}, \tag{41}$$

where the equality follows from (31).

In order to simplify the terminology, we do not call $\mathscr{E}_{\mathrm{ST}}$ the "space-time-algebraic" error but only space-time error, similarly $\mathscr{E}_{\mathrm{S}}$ is not called the "space-algebraic" error but only space error and $\mathscr{E}_{\mathrm{T}}$ is not called the "time-algebraic" error but only time error, although that terminology would be more precise. From (38) – (41), we simply find that

$$\mathscr{E}_{\mathrm{A}}(\tilde{\boldsymbol{w}}_{h\tau}) \le \mathscr{E}_{\mathrm{T}}(\tilde{\boldsymbol{w}}_{h\tau}) \le \mathscr{E}_{\mathrm{ST}}(\tilde{\boldsymbol{w}}_{h\tau}), \quad \mathscr{E}_{\mathrm{A}}(\tilde{\boldsymbol{w}}_{h\tau}) \le \mathscr{E}_{\mathrm{S}}(\tilde{\boldsymbol{w}}_{h\tau}) \le \mathscr{E}_{\mathrm{ST}}(\tilde{\boldsymbol{w}}_{h\tau}), \quad \tilde{\boldsymbol{w}}_{h\tau} \in S^{\tau,q}(\mathcal{I}_\tau; \boldsymbol{S}_{h,p}),$$

which reflects the introduced error definitions.

However, the evaluation of error measures $\mathscr{E}_{\mathrm{ST}}(\tilde{\boldsymbol{w}}_{h\tau})$, $\mathscr{E}_{\mathrm{T}}(\tilde{\boldsymbol{w}}_{h\tau})$ and $\mathscr{E}_{\mathrm{S}}(\tilde{\boldsymbol{w}}_{h\tau})$ is practically impossible since the suprema are taken over infinite dimensional spaces $H^1(\mathcal{I}_\tau, \boldsymbol{H}^2(\mathscr{T}_h))$, $H^1(\mathcal{I}_\tau; \boldsymbol{S}_{h,p})$ and $S^{\tau,q}(\mathcal{I}_\tau; \boldsymbol{H}^2(\mathscr{T}_h))$, respectively. Therefore, in our approach, we seek the maximum over some sufficiently large but finite dimensional subspaces of the spaces mentioned above. Particularly, we employ the spaces

$$S^{\tau,q+1}(\mathcal{I}_\tau; \boldsymbol{S}_{h,p+1}), \qquad S^{\tau,q+1}(\mathcal{I}_\tau; \boldsymbol{S}_{h,p}), \qquad S^{\tau,q}(\mathcal{I}_\tau; \boldsymbol{S}_{h,p+1}), \tag{42}$$

which consist of vector-valued piecewise polynomial functions over $K \times I_m$ of the degree $\le p(+1)$ with respect to $x \in K$ and the degree $\le q(+1)$ with respect to $t \in I_m$ for $K \in \mathscr{T}_{h,m}$ and $I_m \in \mathcal{I}_\tau$.

Let $\tilde{\boldsymbol{w}}_{h\tau}$ be the computed approximate solution. Then based on (38) – (41), we define

$$\eta_{\mathrm{ST}}(\tilde{\boldsymbol{w}}_{h\tau}) := \sup_{\substack{\boldsymbol{\psi}_h\in S^{\tau,q+1}(\mathcal{I}_\tau;\boldsymbol{S}_{h,p+1})\\ \boldsymbol{\psi}_h\neq 0}} \frac{\boldsymbol{A}_{h\tau}(\tilde{\boldsymbol{w}}_{h\tau},\boldsymbol{\psi}_h)}{\|\boldsymbol{\psi}_h\|_X}, \quad \eta_{\mathrm{T}}(\tilde{\boldsymbol{w}}_{h\tau}) := \sup_{\substack{\boldsymbol{\psi}_h\in S^{\tau,q+1}(\mathcal{I}_\tau;\boldsymbol{S}_{h,p})\\ \boldsymbol{\psi}_h\neq 0}} \frac{\boldsymbol{A}_{h\tau}(\tilde{\boldsymbol{w}}_{h\tau},\boldsymbol{\psi}_h)}{\|\boldsymbol{\psi}_h\|_X}, \tag{43}$$

$$\eta_{\mathrm{S}}(\tilde{\boldsymbol{w}}_{h\tau}) := \sup_{\substack{\boldsymbol{\psi}_h\in S^{\tau,q}(\mathcal{I}_\tau;\boldsymbol{S}_{h,p+1})\\ \boldsymbol{\psi}_h\neq 0}} \frac{\boldsymbol{A}_{h\tau}(\tilde{\boldsymbol{w}}_{h\tau},\boldsymbol{\psi}_h)}{\|\boldsymbol{\psi}_h\|_X}, \qquad \eta_{\mathrm{A}}(\tilde{\boldsymbol{w}}_{h\tau}) := \sup_{\substack{\boldsymbol{\psi}_h\in S^{\tau,q}(\mathcal{I}_\tau;\boldsymbol{S}_{h,p})\\ \boldsymbol{\psi}_h\neq 0}} \frac{\boldsymbol{A}_{h\tau}(\tilde{\boldsymbol{w}}_{h\tau},\boldsymbol{\psi}_h)}{\|\boldsymbol{\psi}_h\|_X} = \mathscr{E}_{\mathrm{A}}(\tilde{\boldsymbol{w}}_{h\tau}),$$

which we call *space-time*, *time*, *space* and *algebraic residual error estimators*, respectively.

4.3. Properties of the residual error estimators

Obviously, if $\boldsymbol{w} \in H^1(0,T;\boldsymbol{H}^2(\Omega)) \subset H^1(\mathcal{I}_\tau,\boldsymbol{H}^2(\mathscr{T}_h))$ is the exact solution of (1) then due to the consistency (30) and the fact that the spaces from expression (42) are subspaces of $H^1(\mathcal{I}_\tau,\boldsymbol{H}^2(\mathscr{T}_h))$, we have

$$\eta_{\mathrm{ST}}(\boldsymbol{w}) = \eta_{\mathrm{T}}(\boldsymbol{w}) = \eta_{\mathrm{S}}(\boldsymbol{w}) = \eta_{\mathrm{A}}(\boldsymbol{w}) = 0.$$

Furthermore, we have immediately lower bounds

$$\eta_{\mathrm{ST}}(\tilde{\boldsymbol{w}}_{h\tau}) \le \mathscr{E}_{\mathrm{ST}}(\tilde{\boldsymbol{w}}_{h\tau}), \quad \eta_{\mathrm{T}}(\tilde{\boldsymbol{w}}_{h\tau}) \le \mathscr{E}_{\mathrm{T}}(\tilde{\boldsymbol{w}}_{h\tau}), \quad \eta_{\mathrm{S}}(\tilde{\boldsymbol{w}}_{h\tau}) \le \mathscr{E}_{\mathrm{S}}(\tilde{\boldsymbol{w}}_{h\tau}), \quad \eta_{\mathrm{A}}(\tilde{\boldsymbol{w}}_{h\tau}) = \mathscr{E}_{\mathrm{A}}(\tilde{\boldsymbol{w}}_{h\tau}), \tag{44}$$

since the suprema in the estimates η_* are taken over smaller spaces than the suprema in the error estimates $\mathscr{E}_*$. However, it is open if there exists an upper bound, i.e., $\mathscr{E}_*(\cdot) \le C\eta_*(\cdot)$, where $C > 0$. This will be the subject of future research.

Finally, from (43), we simply find that

$$\eta_{\mathrm{A}}(\tilde{\boldsymbol{w}}_{h\tau}) \le \eta_{\mathrm{T}}(\tilde{\boldsymbol{w}}_{h\tau}) \le \eta_{\mathrm{ST}}(\tilde{\boldsymbol{w}}_{h\tau}), \quad \eta_{\mathrm{A}}(\tilde{\boldsymbol{w}}_{h\tau}) \le \eta_{\mathrm{S}}(\tilde{\boldsymbol{w}}_{h\tau}) \le \eta_{\mathrm{ST}}(\tilde{\boldsymbol{w}}_{h\tau}), \quad \tilde{\boldsymbol{w}}_{h\tau} \in S^{\tau,q}(\mathcal{I}_\tau;\boldsymbol{S}_{h,p}). \tag{45}$$

Remark 4.1. *It would be possible to define space $\boldsymbol{S}_{h,p+1}$ in a different way, e.g., to enrich it by polynomials of even higher degree or introduce some interelement splitting of elements $K \in \mathscr{T}_{h,m}$. However, any further enrichment of $\boldsymbol{S}_{h,p+1}$ requires additional computational time and the numerical experiments show that the presented choice of $\boldsymbol{S}_{h,p+1}$ is sufficient.*

4.4. Evaluation of the residual error estimators

Let $\tilde{\boldsymbol{w}}_{h\tau}$ be the computed approximate solution. In order to simplify the notation in the following, we introduce a generic definition of the residual error estimators (43) by

$$\eta_\star(\tilde{\boldsymbol{w}}_{h\tau}) := \sup_{\substack{\boldsymbol{\psi}_h \in X_h \\ \boldsymbol{\psi}_h \neq 0}} \frac{\boldsymbol{A}_{h\tau}(\tilde{\boldsymbol{w}}_{h\tau},\boldsymbol{\psi}_h)}{\|\boldsymbol{\psi}_h\|_X}, \qquad \star \in \{\mathrm{ST},\mathrm{T},\mathrm{S},\mathrm{A}\}, \tag{46}$$

which formally represents any definition from (43), where X_h denotes the corresponding functional space. We define the *residual error estimates at time interval I_m* by

$$\eta_\star^m(\tilde{\boldsymbol{w}}_{h\tau}) := \sup_{\substack{0 \neq \boldsymbol{\psi}_h \in X_h \\ \mathrm{supp}(\boldsymbol{\psi}_h) \subset \Omega \times I_m}} \frac{\boldsymbol{A}_{h\tau}(\tilde{\boldsymbol{w}}_{h\tau},\boldsymbol{\psi}_h)}{\|\boldsymbol{\psi}_h\|_X}, \qquad m = 1,\dots,r \tag{47}$$

and the *element residual error estimates* by

$$\eta_\star^{m,K}(\tilde{\boldsymbol{w}}_{h\tau}) := \sup_{\substack{0 \neq \boldsymbol{\psi}_h \in X_h \\ \mathrm{supp}(\boldsymbol{\psi}_h) \subset K \times I_m}} \frac{\boldsymbol{A}_{h\tau}(\tilde{\boldsymbol{w}}_{h\tau},\boldsymbol{\psi}_h)}{\|\boldsymbol{\psi}_h\|_X}, \qquad K \in \mathscr{T}_{h,m}, \quad m = 1,\dots,r, \tag{48}$$

which exhibits a "restriction" of the residual error estimators on a time interval and a space-time element, respectively.

Remark 4.2. *Let us note that the value $\eta_\star^m(\tilde{\boldsymbol{w}}_{h\tau})$ depends only on $\tilde{\boldsymbol{w}}_{h\tau}^m := \tilde{\boldsymbol{w}}_{h\tau}|_{I_m\times\Omega}$, cf. (17). Therefore, sometimes we write $\eta_\star^m(\tilde{\boldsymbol{w}}_{h\tau}^m)$ instead of $\eta_\star^m(\tilde{\boldsymbol{w}}_{h\tau})$ and $\eta_\star^{m,K}(\tilde{\boldsymbol{w}}_{h\tau}^m)$ instead of $\eta_\star^{m,K}(\tilde{\boldsymbol{w}}_{h\tau})$.*

The generic definitions (47) and (48) define the (space-time, time, space and algebraic) residual error estimates η_{ST}^m, η_{T}^m, η_{S}^m and η_{A}^m on the time interval I_m, $m = 1,\dots,r$ and the element (space-time, time, space and algebraic) residual error estimates $\eta_{\mathrm{ST}}^{m,K}$, $\eta_{\mathrm{T}}^{m,K}$, $\eta_{\mathrm{S}}^{m,K}$ and $\eta_{\mathrm{A}}^{m,K}$ on element $K \in \mathscr{T}_{h,m}$ and on the time interval I_m, $m = 1,\dots,r$, respectively.

For simplicity, we set $X := H^1(\mathcal{I}_\tau,\boldsymbol{H}^2(\mathscr{T}_h))$. Obviously, $S^{\tau,q}(\mathcal{I}_\tau;\boldsymbol{S}_{h,p}) \subset S^{\tau,q}(\mathcal{I}_\tau;\boldsymbol{S}_{h,p+1}) \subset X$ and $S^{\tau,q}(\mathcal{I}_\tau;\boldsymbol{S}_{h,p}) \subset S^{\tau,q+1}(\mathcal{I}_\tau;\boldsymbol{S}_{h,p}) \subset X$. If the norm $\|\cdot\|_X$ is suitably chosen then the evaluation of $\eta_\star$, $\star \in \{\mathrm{ST},\mathrm{T},\mathrm{S},\mathrm{A}\}$ is cheap. First, we present the following lemma.

Lemma 4.3. *Let $(\cdot,\cdot)_X : X \times X \to \mathbb{R}$ be a scalar product generating the norm $\|\cdot\|_X$. Let $(\cdot,\cdot)_X$ satisfy the* element-orthogonality *condition*

$$(\psi_h, \psi_h')_X = 0 \quad \forall \psi_h, \psi_h' \in X \quad \textit{such that} \quad \operatorname{supp}(\psi_h) \textit{ and } \operatorname{supp}(\psi_h') \textit{ have disjoint interiors.} \tag{49}$$

Then

$$\eta_\star(\tilde{\boldsymbol{w}}_{h\tau})^2 = \sum_{m=1}^{r} \eta_\star^m(\tilde{\boldsymbol{w}}_{h\tau})^2 = \sum_{m=1}^{r} \sum_{K\in\mathscr{T}_{h,m}} \eta_\star^{m,K}(\tilde{\boldsymbol{w}}_{h\tau})^2 \qquad \forall \tilde{\boldsymbol{w}}_{h\tau} \in X_h, \tag{50}$$

where X_h denotes the corresponding finite dimensional space appearing in the definition of $\eta_\star$.

Proof. The proof is analogous to the proof [51, Lemma 4.3]. Let $\boldsymbol{\phi}_{m,K} \in X_h$, $m = 1,\dots,r$, $K \in \mathscr{T}_{h,m}$, $\|\boldsymbol{\phi}_{m,K}\|_X = 1$ denote the functions for which the maximums in (48) are attained, i.e., $\eta_\star^{m,K}(\tilde{\boldsymbol{w}}_{h\tau}) = \boldsymbol{A}_{h\tau}(\tilde{\boldsymbol{w}}_{h\tau}, \boldsymbol{\phi}_{m,K})$. Any function $\boldsymbol{\psi}_h \in X_h$, $\|\boldsymbol{\psi}_h\|_X = 1$ can be rewritten as $\boldsymbol{\psi}_h = \sum_{m=1}^{r}\sum_{K\in\mathscr{T}_{h,m}} c_{m,K}\boldsymbol{\varphi}_{m,K}$, where $\boldsymbol{\varphi}_{m,K}$, $m = 1,\dots,r$, $K \in \mathscr{T}_{h,m}$ are such that $\operatorname{supp}\boldsymbol{\varphi}_{m,K} \subset K \times I_m$ and $\|\boldsymbol{\varphi}_{m,K}\|_X = 1$.

Then, due to (49), $\|\boldsymbol{\psi}_h\|_X^2 = \sum_{m=1}^{r}\sum_{K\in\mathscr{T}_{h,m}} c_{m,K}^2 = 1$. Moreover, using the Cauchy inequality, we have the bound

$$\begin{aligned}\boldsymbol{A}_{h\tau}(\tilde{\boldsymbol{w}}_{h\tau}, \boldsymbol{\psi}_h) &= \sum_{m=1}^{r}\sum_{K\in\mathscr{T}_{h,m}} c_{m,K}\boldsymbol{A}_{h\tau}(\tilde{\boldsymbol{w}}_{h\tau}, \boldsymbol{\varphi}_{m,K}) \le \left(\sum_{m=1}^{r}\sum_{K\in\mathscr{T}_{h,m}} c_{m,K}^2\right)^{1/2}\left(\sum_{m=1}^{r}\sum_{K\in\mathscr{T}_{h,m}} \boldsymbol{A}_{h\tau}(\tilde{\boldsymbol{w}}_{h\tau}, \boldsymbol{\varphi}_{m,K})^2\right)^{1/2}\\ &\le \left(\sum_{m=1}^{r}\sum_{K\in\mathscr{T}_{h,m}} \eta_\star^{m,K}(\tilde{\boldsymbol{w}}_{h\tau})^2\right)^{1/2}, \qquad \boldsymbol{\psi}_h \in X_h,\ \|\boldsymbol{\psi}_h\|_X = 1.\end{aligned}$$

This implies that

$$\eta_\star(\tilde{\boldsymbol{w}}_{h\tau})^2 = \left(\sup_{\substack{\boldsymbol{\psi}_h\in X_h\\ \boldsymbol{\psi}_h\neq 0}} \frac{\boldsymbol{A}_{h\tau}(\tilde{\boldsymbol{w}}_{h\tau}, \boldsymbol{\psi}_h)}{\|\boldsymbol{\psi}_h\|_X}\right)^2 \le \sum_{m=1}^{r}\sum_{K\in\mathscr{T}_{h,m}} \eta_\star^{m,K}(\tilde{\boldsymbol{w}}_{h\tau})^2. \tag{51}$$

On the other hand, we put

$$\bar{\boldsymbol{\psi}}_h := \frac{\sum_{m=1}^{r}\sum_{K\in\mathscr{T}_{h,m}} \boldsymbol{A}_{h\tau}(\tilde{\boldsymbol{w}}_{h\tau}, \boldsymbol{\phi}_{m,K})\,\boldsymbol{\phi}_{m,K}}{(\sum_{m=1}^{r}\sum_{K\in\mathscr{T}_{h,m}} \boldsymbol{A}_{h\tau}(\tilde{\boldsymbol{w}}_{h\tau}, \boldsymbol{\phi}_{m,K})^2)^{1/2}}.$$

Then, due to (49), we have $\|\bar{\boldsymbol{\psi}}_h\|_X = 1$. Finally, a simple calculation gives $\boldsymbol{A}_{h\tau}(\tilde{\boldsymbol{w}}_{h\tau}, \bar{\boldsymbol{\psi}}_h) = \left(\sum_{m=1}^{r}\sum_{K\in\mathscr{T}_{h,m}} \eta_\star^{m,K}(\tilde{\boldsymbol{w}}_{h\tau})^2\right)^{1/2}$ and therefore (51) is valid with the equality, which proves the lemma. The proof of the second equality in (50) is analogous. □

If the norm $\|\cdot\|_X$ satisfies (49) then the global estimators can be evaluated simply be summing of squares of the element estimators, due to (50). Then, it is sufficient to evaluate the element residual error estimators $\eta_\star^{m,K}$, for all $m = 1,\dots,r$ and all $K \in \mathscr{T}_{h,m}$. This is a standard task of seeking a constrained extremum over the finite dimensional space

$$X_h^{K,m} := \{\boldsymbol{\psi}_h \in X_h;\ \operatorname{supp}(\boldsymbol{\psi}_h) \subset K \times I_m\} \subset [P^{p+\delta_p}(K) \times P^{q+\delta_q}(I_m)]^4, \quad K \in \mathscr{T}_{h,m},\ m = 1,\dots,r,$$

where $(\delta_p, \delta_q) \in \{(0,0),\ (0,1),\ (1,0),\ (1,1)\}$. We evaluate the form $\boldsymbol{A}_{h\tau}(\tilde{\boldsymbol{w}}_{h\tau}, \boldsymbol{\psi}_h)$ in (48) for functions $\boldsymbol{\psi}_h$ forming a basis of $X_h^{K,m}$ and then we seek the constrained extremum by the technique of the Lagrange multipliers, see [51, Appendix] for more details. Let us note that the seeking of the constrained extrema is relatively fast in comparison to the other parts of the computational process, see Figure 10 (bottom right) in Section 6.3.

In order to fulfil the favorable property (50), we employ (based on numerical experiments) the scalar product

$$(u,v)_X := \sum_{m=1}^{r} \Big[\int_{I_m} \big[(u,v)_\Omega + \frac{1}{\mathrm{Re}} \sum_{K\in\mathscr{T}_{h,m}} (\nabla u, \nabla v)_K + (\partial_t u, \partial_t v)_\Omega \big] \,\mathrm{d}t \Big], \ u,v \in X, \tag{52}$$

where $(\nabla u, \nabla v)_K = \int_K \nabla u \cdot \nabla v \,\mathrm{d}x$ and Re is the Reynolds number, for inviscid flow we put $1/\mathrm{Re} := 0$. This scalar product satisfies (49) with the corresponding norm

$$\|u\|_X = \left\{ \int_0^T \left[\|u\|^2_{L^2(\Omega)} + \frac{1}{\mathrm{Re}} |u|^2_{\boldsymbol{H}^1(\mathscr{T}_h)} + \|\partial_t u\|^2_{L^2(\Omega)} \right] \mathrm{d}t \right\}^{1/2}, \quad u \in X. \tag{53}$$

The scalar product $(\cdot,\cdot)_X$ and the norm $\|\cdot\|_X$ is the (weighted) broken analogue of the standard norm of the Bochner space $H^1(0,T;H^1(\Omega))$. Obviously, there are many other choices satisfying the element-orthogonality property (49). In Appendix, we present a theoretical justification for the choice (52) – (53).

4.5. An employment of the error estimates in the solution strategy

In Section 3.4, we introduced the solution strategy for the solution of the sequence of the nonlinear algebraic systems given by Definition 3.1 with the aid of the inexact Newton-like method. Two aspects stay open there: the termination of the iterative process (25) – (26) and the choice of the time step. We employ the residual error estimates introduced in previous sections. Again, let $\tilde{\boldsymbol{w}}_{h\tau} \in S^{\tau,q}(\mathcal{I}_\tau; \boldsymbol{S}_{h,p}) \subset H^1(\mathcal{I}_\tau, \boldsymbol{H}^2(\mathscr{T}_h))$ denote the resulting approximate solution of the STDG method (15) computed by the iterative process (25) – (26).

Termination of the iterative process. Using the Newton-like iterative process (25) – (26), we compute the approximations $\tilde{\boldsymbol{w}}^{m,(l)}_{h\tau}$, $l = 1,2,\dots$ of the function $\boldsymbol{w}^m_{h\tau}$. Here, $\tilde{\boldsymbol{w}}^{m,(l)}_{h\tau}$ denotes the piecewise polynomial function corresponding to the vector $\boldsymbol{\xi}^l_m$, $l = 1,2,\dots$ from (25) – (26) by the isomorphism (18). We stop this iterative process if the algebraic residual error estimate at time interval I_m is sufficiently small in comparison to the space residual error estimate at time interval I_m, i.e.,

$$\eta^m_{\mathrm{A}}(\tilde{\boldsymbol{w}}^{m,(l)}_{h\tau}) \le c_A \eta^m_{\mathrm{S}}(\tilde{\boldsymbol{w}}^{m,(l)}_{h\tau}), \quad m = 1,\dots,r, \tag{54}$$

where $0 < c_A < 1$ is a suitable constant which checks a relative influence of the nonlinear algebraic error to the space discretization. It is reasonable to set $c_A \in [10^{-2}, 10^{-1}]$. Hence, we put $\tilde{\boldsymbol{w}}_{h\tau}|_{I_m} := \tilde{\boldsymbol{w}}^{m,(l)}_{h\tau}$ where l is the minimal index satisfying (54).

Choice of the time step in (15). The aim is to choose the time step τ_m such that the time residual error estimate at time interval I_m is controlled by the space residual error estimate at time interval I_m, i.e.,

$$\eta^m_{\mathrm{T}}(\tilde{\boldsymbol{w}}^m_{h\tau}) \le c_T \eta^m_{\mathrm{S}}(\tilde{\boldsymbol{w}}^m_{h\tau}), \quad m = 1,\dots,r, \tag{55}$$

where $c_T > 0$ is a suitable constant representing a desired ratio of the time and space error. Therefore, at each time level $m = 1,\dots,r$, we evaluate estimates $\eta^m_{\mathrm{T}}(\tilde{\boldsymbol{w}}^m_{h\tau})$ and $\eta^m_{\mathrm{S}}(\tilde{\boldsymbol{w}}^m_{h\tau})$ and define the "optimal" time step

$$\tau^{\mathrm{opt}}_m := \tau_m \tilde{c}_T \left(\frac{c_T \eta^m_{\mathrm{S}}(\tilde{\boldsymbol{w}}^m_{h\tau})}{\eta^m_{\mathrm{T}}(\tilde{\boldsymbol{w}}^m_{h\tau})} \right)^{1/(q+1)}, \tag{56}$$

where $\tilde{c}_T \in (0,1)$ is an security factor. In the experiments presented in this paper, we use the value $\tilde{c}_T = 0.9$. Now, if condition (55) is not satisfied we repeat the m^{th}-time step with τ^{opt}_m

instead of τ_m, otherwise we proceed to the $(m+1)^{\text{th}}$-time step with $\tau_{m+1} := \tau_m^{\text{opt}}$. This technique is standard, more details can be found in [46, 47, 52].

For non-stationary flow simulation, it is reasonable to set $c_T \in [10^{-2}, 10^{-1}]$ in order to suppress the influence of the time discretization with respect to the space discretization. On the other hand, when we use the scheme (15) for a steady state simulation with the aid of time stabilization, c_T can be large, e.g., $c_T := 1$, $c_T := 10$ or even higher values. Finally, let us note that numerical experiments showed that parameters c_A and c_T should satisfy $c_A < c_T$ otherwise some instability may appear in the computation due to an insufficient solution of the algebraic systems.

Remark 4.4. *Let us note that it is possible to consider the* local criteria, *when we replace* (54) *and* (55) *by*

$$\eta_{\text{A}}^{m,K} \le c'_A \eta_{\text{S}}^{m,K} \quad \textit{and} \quad \eta_{\text{T}}^{m,K} \le c'_T \eta_{\text{S}}^{m,K} \quad \forall K \in \mathscr{T}_{h,m},\ m = 1, \dots, r, \tag{57}$$

respectively, where $c'_A > 0$ and $c'_T > 0$ are constants. However, based on our experiences, these local criteria are problematic in the situation when the approximate solution is equal (up to a computer precision) to the exact one on some $K \in \mathscr{T}_{h,m}$ (e.g., the flow is constant on elements K which are far from an airfoil). Then we have $\eta_{\text{A}}^{m,K} \approx \eta_{\text{S}}^{m,K} \approx \eta_{\text{T}}^{m,K} \approx 0$ for these elements and thus the local criterion above can not be satisfied.

Remark 4.5.

4.6. Adaptive space-time DG method

It is challenging to develop a full space-time adaptive technique for non-stationary problems. Although the residual error estimators described above do not give an upper error bound, we use them for an adaptive algorithm which adapts (locally) the mesh and (globally) the size of the time step.

The aim is to adapt the mesh and the time step in such a way that the *space-time residual error estimator* η_{ST} is *under a given tolerance* $\omega > 0$, i.e.,

$$\eta_{\text{ST}}(\tilde{\boldsymbol{w}}_{h\tau}) \le \omega. \tag{58}$$

In the computational process, we prescribe the tolerance for the space-time residual error estimates η_{ST}^m on the time interval $I_m,\ m = 1, \dots, r$, namely

$$\eta_{\text{ST}}^m(\tilde{\boldsymbol{w}}_{h\tau}) \le \omega_m, \quad \omega_m := \omega \sqrt{\tau_m / T}, \quad m = 1, \dots, r, \tag{59}$$

where ω_k is the tolerance for the time level $t_k,\ m = 1, \dots, r$. The condition (59) implies (58) due to (50).

Then we define the following *space-time adaptive process*:

(1) let $\omega > 0$ be a given tolerance, $\mathscr{T}_{h,0}$ the initial mesh and τ_0 the initial time step,

(2) $m := 1$,

(3) we solve problem (20) by the iterative method (25) – (26) until the stopping criterion $\eta_{\text{A}}^m \le c_A \eta_{\text{S}}^m$ is satisfied,

(4) if $\eta_{\text{T}}^m > c_T \eta_{\text{S}}^m$ we adapt the time step τ_m according (56) and go to step (3),

(5) if $\eta_{\text{ST}}^m > \omega_m$ then we adapt mesh $\mathscr{T}_{h,m}$ and go to step (3),

(6) if $t_m \ge T$ then the computation finishes,
else we put $\mathscr{T}_{h,m+1} := \mathscr{T}_{h,m}$, $\tau_{m+1} := \tau_m^{\text{opt}}$, $m := m + 1$ and go to step (3).

If condition (59) is violated for some $m = 1, \dots, r$, the mesh $\mathscr{T}_{h,m}$ has to be adapted (step (5) of the algorithm). We use the following mesh adaptation strategy. We require that error estimate has to be equidistributed over Ω, namely

$$\eta_{\mathrm{ST}}^{m,K} \approx \omega_{K,m}, \qquad \text{where } \omega_{K,m} := c_S \omega_m \left(|K|/|\Omega|\right)^{1/2}, \quad K \in \mathscr{T}_{h,m},\ m = 1, \dots, r, \tag{60}$$

and $c_S \in (0,1)$ is a *security factor*, usually chosen $c_S \approx 0.5$. Due to the security factor, we have no troubles to achieve condition (59) after mesh adaptation and moreover, one mesh is usually used for several time steps. Hence, we avoid too often re-meshing which requires some additional computational time.

Numerical experiments presented in Section 5 show that $\eta_{\mathrm{ST}}^{m} = O(h^p)$ (provided that the exact solution is sufficiently accurate) thus the optimal size of the element K denoted by h_K^{opt} is given by

$$h_K^{\mathrm{opt}} := h_K \left(\omega_{K,m}/\eta_{\mathrm{ST}}^{m,K}\right)^{1/p}, \quad K \in \mathscr{T}_{h,m},\ m = 1, \dots, r. \tag{61}$$

This relation follows from the "semi-equalities" $\eta_{\mathrm{ST}}^{m,K} \approx C h_k^p$ and $\omega_{K,m} \approx C(h_K^{\mathrm{opt}})^p$ where $C > 0$ is an undetermined constant which has to be eliminated. In this paper we employ two mesh adaptation techniques:

- *Isotropic mesh adaptation*, where using (61), we set the "optimal" size for each $K \in \mathscr{T}_{h,m}$ which is associated with the barycentre of K. Then we construct (almost) equilateral triangles with the aid of technique of the *anisotropic mesh adaptation*, see, e.g., [53] or the documentation of the used code ANGENER [54].
- *Anisotropic mesh adaptation*, where using (61), we set again the "optimal" size for each $K \in \mathscr{T}_{h,m}$. Moreover, the "anisotropy" of triangles is obtained by the technique based on the interpolation error estimates, see [55]. Then we construct anisotropic mesh again with the aid of technique from [53, 54].

4.7. Choice of the algorithm parameters

5. Numerical verification for scalar convection-diffusion equations

In this section, we present the basic numerical tests demonstrating reasonability of the proposed error estimators η_{A}, η_{S}, η_{T} and η_{ST} given by (43). In virtues of (16), we expect that

$$\begin{aligned} &\text{if } C_1 h^p \ll C_2 \tau^{q+1} \quad \text{then} \quad \eta_{\mathrm{S}} \ll \eta_{\mathrm{T}} \quad \& \quad \eta_{\mathrm{T}} = O(\tau^{q+1}) = \eta_{\mathrm{ST}}, \\ &\text{if } C_1 h^p \gg C_2 \tau^{q+1} \quad \text{then} \quad \eta_{\mathrm{S}} \gg \eta_{\mathrm{T}} \quad \& \quad \eta_{\mathrm{S}} = O(h^p) = \eta_{\mathrm{ST}}, \end{aligned} \tag{62}$$

where C_1 and C_2 are constants from (16). In Sections 5.1 and 5.2, we show that the proposed error estimates fulfil both expectations given by (62). We use the algorithm from Section 4.6 with fixed τ and mesh $\mathscr{T}_h = \mathscr{T}_{h,m},\ m = 0, \dots, r$, i.e., we skip steps (4) and (5). In order to avoid an influence of the inexact solution of algebraic systems, we put $c_A := 10^{-3}$ in step (3) of the algorithm.

Moreover, in Section 5.3, we demonstrate the role of the nonlinear algebraic stopping criterion (54) for a nonlinear convection-diffusion equation. Finally, in Section 5.4, we show the application of the residual error to problem, where the exact solution contains a singularity.

In Sections 5.1 and 5.2, we consider the scalar convection-diffusion equation

$$\frac{\partial u}{\partial t} + \frac{\partial u}{\partial x_1} - \varepsilon \Delta u = f \qquad \text{in } \Omega \times (0,T) = (0,1)^2 \times (0,1/2), \tag{63}$$

where $\varepsilon = 0.1$ is the diffusion coefficient. We add the initial and the Dirichlet boundary condition on $\partial\Omega$ such that the exact solution has the form

$$u(x_1, x_2, t) = (\delta + e^{\alpha t}) x_1 x_2 (1 - x_1)(1 - x_2), \tag{64}$$

where $\delta, \alpha \in \mathbb{R}$ are parameters. These parameters are set separately for demonstration of both implications in (62).

h	τ	p	q	$\|e_{h\tau}\|_{L^2(H^1)}$	η_A	η_S	η_T	η_{ST}	i_X
1/16	1/10	4	1	2.632E-01	7.106E-10	2.128E-06	5.414E-02	5.414E-02	2.057E-01
1/16	1/20	4	1	6.427E-02	2.903E-10	6.006E-07	1.363E-02	1.363E-02	2.121E-01
	(EOC)			(2.03)	(1.29)	(1.83)	(1.99)	(1.99)	
1/16	1/40	4	1	1.570E-02	8.497E-11	1.528E-07	3.377E-03	3.377E-03	2.150E-01
	(EOC)			(2.03)	(1.77)	(1.97)	(2.01)	(2.01)	
1/16	1/80	4	1	3.871E-03	8.778E-11	3.447E-08	8.379E-04	8.379E-04	2.164E-01
	(EOC)			(2.02)	(-0.05)	(2.15)	(2.01)	(2.01)	
1/16	1/10	4	2	1.974E-02	1.517E-10	1.905E-07	3.746E-03	3.746E-03	1.897E-01
1/16	1/20	4	2	2.452E-03	1.314E-10	2.974E-08	4.767E-04	4.767E-04	1.944E-01
	(EOC)			(3.01)	(0.21)	(2.68)	(2.97)	(2.97)	
1/16	1/40	4	2	3.020E-04	1.132E-10	3.787E-09	5.939E-05	5.939E-05	1.966E-01
	(EOC)			(3.02)	(0.22)	(2.97)	(3.00)	(3.00)	
1/16	1/80	4	2	3.735E-05	1.206E-10	3.901E-10	7.387E-06	7.387E-06	1.977E-01
	(EOC)			(3.02)	(-0.09)	(3.28)	(3.01)	(3.01)	
1/16	1/10	4	3	1.162E-03	1.245E-10	1.293E-08	2.042E-04	2.042E-04	1.756E-01
1/16	1/20	4	3	7.316E-05	1.461E-10	9.334E-10	1.309E-05	1.309E-05	1.790E-01
	(EOC)			(3.99)	(-0.23)	(3.79)	(3.96)	(3.96)	
1/16	1/40	4	3	4.532E-06	1.925E-10	1.984E-10	8.186E-07	8.186E-07	1.806E-01
	(EOC)			(4.01)	(-0.40)	(2.23)	(4.00)	(4.00)	
1/16	1/80	4	3	2.811E-07	7.755E-11	7.755E-11	5.100E-08	5.100E-08	1.814E-01
	(EOC)			(4.01)	(1.31)	(1.36)	(4.00)	(4.00)	

Table 1: Scalar equation (63) – (64) with $\delta = 0.1$ and $\alpha = 10$: the value of error $\|e_{h\tau}\|_{L^2(H^1)}$, residual error estimators η_{A}, η_{S}, η_{T}, η_{ST} and $i_X := \eta_{\mathrm{ST}}/\|e_{h\tau}\|_{L^2(H^1)}$.

5.1. Order of convergence with respect to the time variable

In order to verify the order of convergence with respect to time variable, we need an "overkill" of the space discretization. We put $\delta = 0.1$ and $\alpha = 10$ in (64). The solution u is a quartic function for any $t \in [0, T]$ and it is exponentially increasing with respect to t for any $x \in \Omega$. Therefore, we use the $p = 4$ polynomial approximation with respect to space on the uniform grid with the mesh step $h = 1/12$. We employ the P_q, $q = 1, 2, 3$ polynomial approximation with respect to time with fixed time steps $\tau = 1/10,\ 1/20,\ 1/40$ and $1/80$. Table 1 shows the values of the computational error in the (broken) $L^2(H^1)$-seminorm given by

$$\|e_{h\tau}\|_{L^2(H^1)} := \left(\sum_{m=1}^{r} \int_{I_m} \left(\sum_{K \in \mathscr{T}_{h,m}} \int_K |\nabla u(x,t) - \nabla u_{h\tau}(x,t)|^2 \,\mathrm{d}x \right) \,\mathrm{d}t \right)^{1/2} \tag{65}$$

and the values of η_{A}, η_{S}, η_{T} and η_{ST} given by (43). Moreover, we evaluate the ratio $i_X := \eta_{\mathrm{ST}}/\|e_{h\tau}\|_{L^2(H^1)}$. Let us note that i_X is not the standard effectivity index since η_{ST} approximate the error measure in the dual norm. Furthermore, for each q, we evaluate the *experimental order of convergence* (EOC) with respect to τ.

We observe that

- order of convergence of the computational error in the $L^2(H^1)$-seminorm is $O(\tau^{q+1})$,
- the space estimator η_{S} is negligible in comparison to the time estimator η_{T},
- the time estimator $\eta_{\mathrm{T}} = O(\tau^{q+1})$, i.e., the same order as $\|e_{h\tau}\|_{L^2(H^1)}$,
- the index i_X is independent of τ and slightly dependent on q.

Hence, the first implication in (62) is confirmed.

5.2. Order of convergence with respect to the space variables

In order to verify the order of convergence with respect to the space variables, we need an "overkill" of the time discretization. We put $\delta = 1$ and $\alpha = -10$. The solution u is a quartic function for any $t \in [0, T]$ and it is exponentially decreasing with respect to t for any $x \in \Omega$. We use

h	τ	p	q	$\|e_{h\tau}\|_{L^2(H^1)}$	η_A	η_S	η_T	η_{ST}	i_X
1/8	1/20	1	2	2.409E-02	7.815E-06	1.176E-02	8.871E-06	1.176E-02	4.881E-01
1/16	1/20	1	2	1.217E-02	4.431E-06	5.866E-03	4.601E-06	5.866E-03	4.818E-01
	(EOC)			(0.98)	(0.82)	(1.00)	(0.95)	(1.00)	
1/32	1/20	1	2	6.114E-03	6.216E-07	2.936E-03	6.971E-07	2.936E-03	4.802E-01
	(EOC)			(0.99)	(2.83)	(1.00)	(2.72)	(1.00)	
1/8	1/20	2	2	1.557E-03	4.055E-07	6.372E-04	4.471E-07	6.372E-04	4.093E-01
1/16	1/20	2	2	3.936E-04	5.982E-08	1.613E-04	6.632E-08	1.613E-04	4.099E-01
	(EOC)			(1.98)	(2.76)	(1.98)	(2.75)	(1.98)	
1/32	1/20	2	2	9.891E-05	2.474E-08	4.063E-05	2.503E-08	4.063E-05	4.108E-01
	(EOC)			(1.99)	(1.27)	(1.99)	(1.41)	(1.99)	
1/8	1/20	3	2	6.258E-05	2.688E-09	1.924E-05	3.050E-09	1.924E-05	3.075E-01
1/16	1/20	3	2	7.795E-06	4.401E-10	2.369E-06	4.590E-10	2.369E-06	3.039E-01
	(EOC)			(3.01)	(2.61)	(3.02)	(2.73)	(3.02)	
1/32	1/20	3	2	9.731E-07	1.675E-10	2.945E-07	1.677E-10	2.945E-07	3.026E-01
	(EOC)			(3.00)	(1.39)	(3.01)	(1.45)	(3.01)	

Table 2: Scalar equation (63) – (64) with $\delta = 1$ and $\alpha = -10$: the value of error $\|e_{h\tau}\|_{L^2(H^1)}$, residual error estimators η_{A}, η_{S}, η_{T}, η_{ST} and $i_X := \eta_{\mathrm{ST}}/\|e_{h\tau}\|_{L^2(H^1)}$.

the $q = 2$ polynomial approximation with respect to time with the fixed time step $\tau = 1/20$. We perform the computations with the aid of P_p, $p = 1, 2, 3$ polynomial approximation with respect to time on the uniform grids with the mesh steps $h = 1/8$, $1/16$ and $1/32$.

Table 2 shows the values of the computational error in the $L^2(H^1)$-seminorm, the values of η_{A}, η_{S}, η_{T} and η_{ST} given by (43) and the ratio i_X. Furthermore, for each p, we evaluate the *experimental order of convergence* (EOC) with respect to h.

We observe that

- order of convergence of the computational error in the $L^2(H^1)$-seminorm is $O(h^p)$,
- the time estimator η_{T} is negligible in comparison to the space estimator η_{S},
- the space estimator $\eta_{\mathrm{S}} = O(h^p)$, i.e., the same order as $\|e_{h\tau}\|_{L^2(H^1)}$,
- the index i_X is independent of h and slightly dependent on p.

Hence, the second implication in (62) is confirmed.

5.3. Verification of the stopping criterion (54)

In this section we demonstrate the role of the nonlinear algebraic stopping criterion (54). We consider the scalar nonlinear convection-diffusion equation

$$\frac{\partial u}{\partial t} - \nabla \cdot (\boldsymbol{K}(u)\nabla u) - \frac{\partial u^2}{\partial x_1} - \frac{\partial u^2}{\partial x_2} = g \quad \text{in } \Omega \times (0,T) := (0,1)^2 \times (0,1/2), \tag{66}$$

where $\boldsymbol{K}(u)$ is the nonsymmetric matrix given by

$$\boldsymbol{K}(u) = \frac{1}{10}\begin{pmatrix} 2 + \arctan(u) & (2 - \arctan(u))/4 \\ 0 & (4 + \arctan(u))/2 \end{pmatrix}. \tag{67}$$

We prescribe a Dirichlet boundary condition on $\partial\Omega$ and set the source term g such that the exact solution is (64) with $\delta = 0.1$ and $\alpha = 10$.

We use fixed $\tau = 0.1$ and mesh $\mathscr{T}_h = \mathscr{T}_{h,m}$, $m = 0, \ldots, r$ with $h = 1/32$, $p = q = 1$ in (15). In step (3) of the algorithm from Section 4.6, we put $c_A := 2^{-l}$, $l = 0, \ldots, 9$ and investigate the dependence of the computational error and the error estimates on c_A. Table 3 shows the values of the computational error in the $L^2(H^1)$-seminorm, the values of η_{A}, η_{S}, η_{T} and η_{ST} given by (43), the ratio $i_A := \eta_{\mathrm{A}}/\eta_{\mathrm{S}}$ and total computational time in seconds.

We observe that

c_A	$\|e_{h\tau}\|_{L^2(H^1)}$	η_A	η_S	η_T	η_{ST}	i_A	CPU(s)
1/1	7.984E-01	3.054E+01	3.054E+01	3.054E+01	3.054E+01	9.999E-01	5.8
1/2	3.060E-01	2.527E-01	6.832E-01	2.598E-01	6.859E-01	3.698E-01	14.5
1/4	3.054E-01	6.264E-02	6.393E-01	8.676E-02	6.421E-01	9.799E-02	15.6
1/8	3.053E-01	5.254E-02	6.384E-01	7.972E-02	6.412E-01	8.230E-02	17.1
1/16	3.056E-01	8.521E-03	6.365E-01	6.060E-02	6.393E-01	1.339E-02	17.7
1/32	3.056E-01	1.378E-02	6.366E-01	6.159E-02	6.394E-01	2.165E-02	21.0
1/64	3.057E-01	3.066E-03	6.365E-01	6.011E-02	6.393E-01	4.818E-03	21.2
1/128	3.057E-01	1.760E-03	6.365E-01	6.006E-02	6.393E-01	2.765E-03	22.5
1/256	3.057E-01	1.755E-03	6.365E-01	6.006E-02	6.393E-01	2.758E-03	23.7
1/512	3.057E-01	3.989E-04	6.365E-01	6.003E-02	6.393E-01	6.267E-04	24.9

Table 3: Scalar equation (66)–(67) with the exact solution (64) ($\delta = 0.1$ and $\alpha = 10$): the value of error $\|e_{h\tau}\|_{L^2(H^1)}$, residual error estimators η_{A}, η_{S}, η_{T}, η_{ST}, $i_A := \eta_{\mathrm{A}}/\eta_{\mathrm{S}}$ and total computational time in seconds.

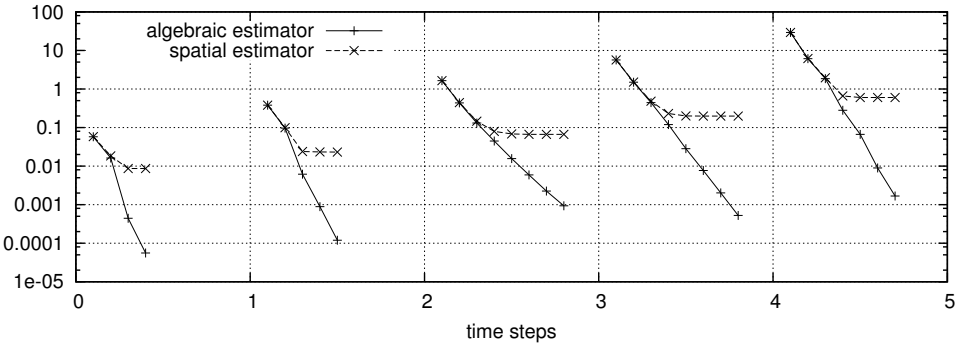

Figure 3: Convergence of the Newton approximations $\tilde{\boldsymbol{w}}_{h\tau}^{m,(l)}$, $l = 1, 2, \ldots$ of $\boldsymbol{w}_{h\tau}^{m}$ within each time step $m = 1, \ldots, 5$, space residual estimator $\eta_{\mathrm{S}}^{m}(\tilde{\boldsymbol{w}}_{h\tau}^{m,(l)})$ and algebraic residuum estimator $\eta_{\mathrm{A}}^{m}(\tilde{\boldsymbol{w}}_{h\tau}^{m,(l)})$.

- using higher values of c_A, the inexactness of the iterative solution of the system of the nonlinear algebraic equations pollutes the error $\|e_{h\tau}\|_{L^2(H^1)}$ and η_{S}; for $c_A \leq 1/16$ this influence is already negligible,
- since the setting of the computation leads to domination of the space error over the time one, the time estimator η_{T} is non-negligibly influenced by the algebraic error for $c_A \geq 1/64$,
- smaller value of c_A leads to higher number of Newton iterations in (25) – (26) and therefore higher computational time.

Moreover, Figure 3 shows a typical convergence of the Newton approximations $\tilde{\boldsymbol{w}}_{h\tau}^{m,(l)}$, $l = 1, 2, \ldots$ of $\boldsymbol{w}_{h\tau}^{m}$ within each time step $m = 1, \ldots, 5$. Namely we present the values of the space residual estimator $\eta_{\mathrm{S}}^{m}(\tilde{\boldsymbol{w}}_{h\tau}^{m,(l)})$ and the algebraic residuum estimator $\eta_{\mathrm{A}}^{m}(\tilde{\boldsymbol{w}}_{h\tau}^{m,(l)})$ obtained with the setting $c_A = 1/512$. We find that after several Newton iterations the value $\eta_{\mathrm{S}}^{m}(\tilde{\boldsymbol{w}}_{h\tau}^{m,(l)})$ is almost constant which means that the spatial error is only negligibly influenced by the algebraic error. Therefore, it would be possible to stop the Newton-like iterative process earlier (with larger c_A) without the lost of the accuracy.

5.4. Problems with non-regular solution

In this section we investigate the behaviour of the proposed error estimates for a problem whose exact solution has a singularity. We consider the nonlinear convection-diffusion equation (66)–(67), where we prescribe the initial and the Dirichlet boundary condition and set the source term g such that the exact solution has the form

$$u(x_1, x_2, t) = (1 - e^{-t})(x_1^2 + x_2^2)^{\beta/2} x_1 x_2 (1 - x_1)(1 - x_2), \tag{68}$$

h	τ	p	q	$\|e_{h\tau}\|_{L^2(H^1)}$	η_A	η_S	η_T	η_{ST}	i_X
1/8	adapt	1	2	9.847E-02	3.141E-05	5.667E-02	3.181E-05	5.667E-02	5.756E-01
1/16	adapt	1	2	7.050E-02	1.126E-05	3.983E-02	1.383E-05	3.983E-02	5.650E-01
	(EOC)			(0.48)	(1.48)	(0.51)	(1.20)	(0.51)	
1/32	adapt	1	2	5.003E-02	1.202E-05	2.800E-02	4.900E-05	2.800E-02	5.596E-01
	(EOC)			(0.49)	(-0.09)	(0.51)	(-1.82)	(0.51)	
1/64	adapt	1	2	3.542E-02	5.012E-06	1.972E-02	4.564E-05	1.972E-02	5.567E-01
	(EOC)			(0.50)	(1.26)	(0.51)	(0.10)	(0.51)	
1/8	adapt	2	2	4.731E-02	5.436E-06	2.336E-02	1.682E-05	2.336E-02	4.938E-01
1/16	adapt	2	2	3.341E-02	1.014E-05	1.665E-02	4.159E-05	1.665E-02	4.983E-01
	(EOC)			(0.50)	(-0.90)	(0.49)	(-1.31)	(0.49)	
1/32	adapt	2	2	2.363E-02	1.019E-05	1.186E-02	1.523E-05	1.186E-02	5.020E-01
	(EOC)			(0.50)	(-0.01)	(0.49)	(1.45)	(0.49)	
1/64	adapt	2	2	1.673E-02	6.734E-06	8.442E-03	3.646E-05	8.442E-03	5.045E-01
	(EOC)			(0.50)	(0.60)	(0.49)	(-1.26)	(0.49)	
1/8	adapt	3	2	4.311E-02	3.702E-06	1.296E-02	2.074E-05	1.296E-02	3.006E-01
1/16	adapt	3	2	3.048E-02	7.447E-06	9.285E-03	3.246E-05	9.285E-03	3.046E-01
	(EOC)			(0.50)	(-1.01)	(0.48)	(-0.65)	(0.48)	
1/32	adapt	3	2	2.155E-02	1.965E-06	6.621E-03	9.811E-06	6.621E-03	3.072E-01
	(EOC)			(0.50)	(1.92)	(0.49)	(1.73)	(0.49)	
1/64	adapt	3	2	1.526E-02	1.942E-06	4.709E-03	1.551E-05	4.709E-03	3.086E-01
	(EOC)			(0.50)	(0.02)	(0.49)	(-0.66)	(0.49)	

Table 4: Scalar equation (66)–(67) with the exact solution (68) ($\beta = -3/2$): the value of error $\|e_{h\tau}\|_{L^2(H^1)}$, residual error estimators $\eta_{\rm A}$, $\eta_{\rm S}$, $\eta_{\rm T}$, $\eta_{\rm ST}$, and $i_A := \eta_{\rm A}/\eta_{\rm S}$.

where we put $\beta = -3/2$. It is possible to show (see [56]) that $u \in H^\kappa(\Omega)$, $\kappa \in (0,\, 3+\beta)$. Therefore, the choice $\beta = -3/2$ leads to the solution with a singularity at $x_1 = x_2 = 0$. Numerical examples presented in [57], carried out for a time-independent problem, show that this singularity avoids to achieve the order of convergence better than $O(h^{1/2})$ in the H^1-seminorm for any degree of polynomial approximation.

We use the presented space-time adaptive process from Section 4.6 with settings $c_A = 10^{-3}$, $c_T = 10^{-2}$ and $q = 2$ (piecewise quadratic approximation with respect to time). We carry out computations using P_1, P_2 and P_3 approximation with respect to space and meshes $\mathscr{T}_h = \mathscr{T}_{h,m},\ m = 0, \dots, r$ with the mesh steps $h = 1/8$, $1/16$, $1/32$ and $1/64$. Table 4 shows the values of the computational error in the $L^2(H^1)$-seminorm, the values of $\eta_{\rm A}$, $\eta_{\rm S}$, $\eta_{\rm T}$ and $\eta_{\rm ST}$ given by (43) and the ratio $i_X = \eta_{\rm ST}/\|e_{h\tau}\|_{L^2(H^1)}$.

We observe that

- order of convergence of the computational error in the $L^2(H^1)$-seminorm is $O(h^{1/2})$ which is in agreement with theoretical results (16),
- the time estimator $\eta_{\rm T}$ is negligible in comparison to the space estimator $\eta_{\rm S}$ since we use $c_T = 10^{-2}$ in (55),
- the space estimator $\eta_{\rm S} = O(h^{1/2})$, i.e., the same order as $\|e_{h\tau}\|_{L^2(H^1)}$,
- the index i_X is independent of h and slightly dependent on p.

6. Numerical experiments for compressible flows

In this section, we present numerical experiments which demonstrate the computational performance of the STDG scheme (15) for the compressible flow problems problem (1) and the residual error estimators (43). In Section 6.1, we consider the propagation of an isentropic vortex, where the exact solution is known. Hence, we can compare the values of the residual error estimates with the computational error. In Section 6.2, we deal with a viscous subsonic flow around NACA0012 profile. This case was treated in several papers (including our former results) as a steady state flow problems. However, we show that a sufficient accurate resolution with respect to time leads to an unsteady flow. In Section 6.3, we present a simulation of viscous shock-vortex interaction, which is more challenging due to a combination of two physical features. Due to the proposed adaptive algorithm, we are able to capture physical features with a reasonable number of degrees of freedom.

6.1. Isentropic vortex propagation

We consider the propagation of an isentropic vortex in compressible inviscid flow, analysed numerically in [58]. This example is suitable for the demonstration of the performance of the proposed residual error estimators since the regular exact solution is known and thus we can simply evaluate the computational error. Then we are able to identify the influence of the space and time discretization parameters h and τ, respectively, to the total computational error.

The computational domain is taken as $[0,10]\times[0,10]$, extended periodically in both directions. The mean flow is $\rho = 1$, $\boldsymbol{v} = (1,1)$ (diagonal flow) and $\mathtt{p} = 1$ (symbol $\mathtt{p}$ denotes the pressure of the flow whereas p denotes the degree of polynomial approximation). To this mean flow we add an *isentropic vortex*, i.e. perturbation in $\boldsymbol{v}$ and the temperature $\theta = \mathtt{p}/\rho$, but no perturbation in the entropy $\eta = \mathtt{p}/\rho^\gamma$:

$$\delta\boldsymbol{v} = \frac{\varepsilon}{2\pi}\exp[(1-r^2)/2](-\bar{x}_2,\bar{x}_1), \quad \delta\theta = -\frac{(\gamma-1)\varepsilon^2}{8\gamma\pi^2}\exp[1-r^2], \quad \delta\eta = 0, \tag{69}$$

where $(-\bar{x}_2,\bar{x}_1) = (x_1-5, x_2-5)$, $r^2 = x_1^2+x_2^2$, and the vortex strength $\varepsilon = 5$. The perturbations $\delta\rho$ and $\delta\mathtt{p}$ are obtained from the above relations.

It is clear that the exact solution of the Euler equations with the initial conditions

$$\rho(x,0) = \bar{\rho} + \delta\rho, \quad \boldsymbol{v}(x,0) = \bar{\boldsymbol{v}} + \delta\boldsymbol{v}, \quad \mathtt{p}(x,0) = \bar{\mathtt{p}} + \delta\mathtt{p}, \tag{70}$$

and periodic boundary conditions is just the passive convection of the vortex with the mean velocity. Therefore, we are able to evaluate the computational error $e_{h\tau} := \boldsymbol{w} - \tilde{\boldsymbol{w}}_{h\tau}$ over the space-time domain $Q_T := \Omega\times(0,T)$, where $\boldsymbol{w}$ is the exact solution of (1) and $\tilde{\boldsymbol{w}}_{h\tau} \in S^{\tau,q}(\mathcal{I}_\tau;\boldsymbol{S}_{h,p})$ is the corresponding approximate solution, namely the output of the Newton-like iterative process (25) – (26). We evaluate $\|e_{h\tau}\|$ in the $L^2(0,T;\boldsymbol{H}^1(\mathscr{T}_h))$-seminorm, cf. (65) and we put the final time $T = 10$ (1 period in time).

We present three types of numerical experiments:

- *fix h + fix τ*: We use two (fixed) unstructured quasi-uniform triangular grid with $\#\mathscr{T}_h = 580$ and $\#\mathscr{T}_h = 2\,484$ triangles with $h \approx 0.894$ and $h \approx 0.448$, respectively, with fixed time steps $\tau = 0.2$, 0.1, 0.05 and 0.025. The simulation was performed with the aid of the STDG scheme (15) for $p = 1$, $p = 2$ and $p = 3$ polynomial approximation with respect to space and for $q = 1$ and $q = 2$ polynomial approximation with respect to time. In order to suppress the influence of the nonlinear algebraic error we set $c_A := 10^{-3}$ in (54).

- *fix h + adapt τ*: We use the same triangular grid but the time step is chosen adaptively according (56) with $c_T = 10^{-2}$ and (54) with $c_A = 10^{-3}$. Again we use $p = 1$, $p = 2$ and $p = 3$ for the space and $q = 1$ and $q = 2$ for the time approximations.

- *adapt h + adapt τ*: We employ the full (space-time) adaptive algorithm from Section 4.6 with tolerances $\omega = 0.04$, $\omega = 0.01$ and 0.0025. We use $p = 3$ approximation in space and $q = 2$ approximation in time. We set $c_T = 10^{-1}$ in (56) and $C_T = 10^{-2}$ in (54). The mesh was adapted by the isotropic as well as anisotropic technique. Since this problem is isotropic the anisotropic techniques can not give essentially better results than the isotropic one.

Table 5 shows the value of errors $\|e_{h\tau}\|_{L^2(H^1)}$, the residual error estimators η_{A}, η_{S}, η_{T}, η_{ST}, the ratio $\eta_{\mathrm{T}}/\eta_{\mathrm{S}}$ and the computational time. The computations where $\eta_{\mathrm{T}}/\eta_{\mathrm{S}} \le 0.01$ are bolted. From these results, we observe the following facts:

- Generally, higher degree of DG method p and q give smaller computational errors.

- The estimator η_{S} is almost independent of τ and the estimator η_{T} decreases for a decreasing τ.

- For each mesh and each pair (p, q), $p = 1, 2, 3$, $q = 2, 3$ there exists a limit value $\bar{\tau}$ such that for any time step $\tau < \bar{\tau}$ we obtain (almost) the same computational error as for $\bar{\tau}$. (For the pair $p = 3$ and $q = 1$ on the finer grid this limit value is lower than all tested τ). It means that (from a practical point of view) the temporal error is negligible compared to the spatial one. Obviously, the limit value $\bar{\tau}$ is larger for large q and it is lower for finer grids and higher p.

- The condition $\eta_{\mathrm{T}}/\eta_{\mathrm{S}} \leq 10^{-2}$ looks like as a reasonable detection if the corresponding time step τ is bellow the limit value $\bar{\tau}$. We can easily observe that the computational errors almost do not change for the bolted lines in the first part of Table 5, an exception is the first case $p = 1$, $q = 1$ and the coarser grid.

- The use of the condition $\eta_{\mathrm{T}}/\eta_{\mathrm{S}} \leq 10^{-2}$ for the adaptive choice of the time step (computations *fix* h + *adapt* τ) leads to approximately same values of $e_{h\tau}$ as the fixed time step but generally with lower computational time. Hence, the time step adaptation keeps the accuracy but increases the efficiency.

- It is also interesting to observe that the *fix* h + *adapt* τ computation with pair $(p = 3, q = 2)$ is faster than the computations with $(p = 3, q = 1)$ although the number of degrees of freedom is higher. This is caused by the fact that $q = 2$ is more accurate with respect time and thus we used smaller number of time steps, which fully compensate the computational costs.

- The full adaptive computations (*adapt* h + *adapt* τ) are able to achieve the same computational error within a shorter computational time. However, in this case the main benifit follows from the weaker conditions (54) and (56) (higher values c_A and c_T). The mesh refinement is not too essential in this case. Nevertheless, these computations show that the space-time DG method as well as the proposed residual error estimates are able to work with different meshes on different time levels. This is well documeneted by the index $i_X := \eta_{\mathrm{ST}}/\|e_{h\tau}\|_{L^2(H^1)}$ in the last part of Table 5 which is not too much varying for different tolerances ω and both mesh adaptation techniques.

Figure 4 shows the grids generated by both mesh adaptation techniques for all tolerances at final time $t = 10$. The solutions obtained by both mesh adaptive techniques are almost identical, hence we show only the isolines of the Mach number obtained by the isotropic adaptation technique. Finally, Figure 5 shows the grids and the Mach number isolines obtained by the anisotropic mesh adaptation at time levels $t = 2.5$, $t = 5.0$ and 7.5. A propagation through the periodical boundaries are observed. Let us note that results obtained by the isotropic mesh adaptation are very similar.

6.2. Viscous subsonic flow

Similarly as in [12, 5, 35, 13], we consider a laminar viscous subsonic flow around the NACA 0012 profile with inlet Mach number $M_{\mathrm{inlet}} = 0.5$, angle of attack $\alpha = 2^\circ$ and Reynolds number $\mathrm{Re} = 5\,000$. In [12, 35], we presented steady-state solutions for this flow regime with several degrees of polynomial approximation with several grids. We employ a relatively coarse unstructured grid having 1 442 triangles, see Figure 6. We carry out computations with the $p = 3$ and $q = 2$ polynomial approximations with respect to space and time, respectively. We employ the computations with $c_T = 10$, $c_T = 0.1$, $c_T = 0.01$, $c_T = 0.005$ and $c_T = 0.002$ in (55).

Figure 7 shows the convergence of the steady-state residuum and the corresponding value of τ_k for all settings of c_T. For $c_T \geq 0.01$, we obtain the steady-state solution. On the other hand, for $c_T = 0.005$ and $c_T = 0.002$, where we have a higher resolution in time, we obtain a non-stationary solution. Moreover, Figure 8 shows the dependence of the lift coefficient c_L on the dimensionless physical time with $c_T = 0.005$ (for $c_T = 0.002$ the results are similar). The constant value c_L-"steady" (= 0.0353) was obtained with the same method but with $c_T = 10$, $c_T = 0.1$ and as well as $c_T = 0.01$. Finally, Figure 9 shows the isolines of the Mach number for $c_T = 10$ and $c_T = 0.005$.

fixed mesh: $\#\mathscr{T}_h = 580$, $h \approx 0.894$

p	q	τ	$\|e_{h\tau}\|_{L^2(H^1)}$	η_A	η_S	η_T	η_{ST}	η_T/η_S	CPU(s)
1	1	2.0E-01	3.38E+00	6.41E-03	1.34E+01	1.15E-01	1.34E+01	**8.57E-03**	85.1
1	1	1.0E-01	3.28E+00	8.13E-03	1.36E+01	3.07E-02	1.36E+01	**2.26E-03**	149.5
1	1	5.0E-02	3.27E+00	4.27E-03	1.36E+01	8.66E-03	1.36E+01	**6.36E-04**	232.8
1	1	2.5E-02	3.26E+00	3.74E-03	1.36E+01	4.20E-03	1.36E+01	**3.08E-04**	369.6
1	2	2.0E-01	3.26E+00	6.23E-03	1.35E+01	8.91E-03	1.35E+01	**6.61E-04**	161.5
1	2	1.0E-01	3.26E+00	5.91E-03	1.36E+01	6.02E-03	1.36E+01	**4.43E-04**	264.3
1	2	5.0E-02	3.26E+00	3.99E-03	1.36E+01	3.99E-03	1.36E+01	**2.93E-04**	409.9
1	2	2.5E-02	3.26E+00	3.60E-03	1.36E+01	3.60E-03	1.36E+01	**2.64E-04**	643.8
2	1	2.0E-01	9.47E-01	1.14E-03	2.23E+00	1.23E-01	2.23E+00	5.50E-02	275.0
2	1	1.0E-01	7.33E-01	1.26E-03	2.31E+00	3.15E-02	2.31E+00	1.37E-02	450.3
2	1	5.0E-02	7.14E-01	1.52E-03	2.32E+00	8.07E-03	2.32E+00	**3.48E-03**	909.9
2	1	2.5E-02	7.12E-01	1.03E-03	2.33E+00	2.24E-03	2.33E+00	**9.61E-04**	1315.7
2	2	2.0E-01	7.13E-01	9.77E-04	2.29E+00	5.48E-03	2.29E+00	**2.40E-03**	757.8
2	2	1.0E-01	7.11E-01	1.30E-03	2.32E+00	1.49E-03	2.32E+00	**6.44E-04**	1157.9
2	2	5.0E-02	7.11E-01	1.20E-03	2.32E+00	1.21E-03	2.32E+00	**5.19E-04**	2136.0
2	2	2.5E-02	7.11E-01	8.64E-04	2.33E+00	8.64E-04	2.33E+00	**3.72E-04**	3194.9
3	1	2.0E-01	5.32E-01	1.71E-04	3.22E-01	1.23E-01	3.45E-01	3.81E-01	1145.1
3	1	1.0E-01	1.59E-01	1.67E-04	3.45E-01	3.16E-02	3.47E-01	9.14E-02	1658.8
3	1	5.0E-02	1.31E-01	1.84E-04	3.50E-01	7.95E-03	3.51E-01	2.27E-02	3030.9
3	1	2.5E-02	1.30E-01	2.07E-04	3.51E-01	2.00E-03	3.51E-01	**5.69E-03**	6058.9
3	2	2.0E-01	1.31E-01	1.54E-04	3.41E-01	5.40E-03	3.41E-01	1.58E-02	2902.7
3	2	1.0E-01	1.30E-01	1.56E-04	3.49E-01	7.08E-04	3.49E-01	**2.03E-03**	4626.3
3	2	5.0E-02	1.30E-01	1.74E-04	3.51E-01	1.95E-04	3.51E-01	**5.56E-04**	8641.0
3	2	2.5E-02	1.30E-01	1.74E-04	3.52E-01	1.75E-04	3.52E-01	**4.96E-04**	15768.9
1	1	adapt	3.40E+00	8.13E-03	1.33E+01	1.29E-01	1.33E+01	**9.65E-03**	83.4
1	2	adapt	3.36E+00	5.69E-03	1.26E+01	1.16E-01	1.26E+01	**9.20E-03**	76.3
2	1	adapt	7.25E-01	1.24E-03	2.31E+00	2.26E-02	2.31E+00	**9.75E-03**	563.0
2	2	adapt	7.31E-01	8.67E-04	2.23E+00	2.07E-02	2.23E+00	**9.31E-03**	668.9
3	1	adapt	1.30E-01	1.82E-04	3.51E-01	3.44E-03	3.51E-01	**9.79E-03**	4404.1
3	2	adapt	1.30E-01	1.75E-04	3.44E-01	3.22E-03	3.44E-01	**9.35E-03**	3782.0

fixed mesh: $\#\mathscr{T}_h = 2\,484$, $h \approx 0.448$

p	q	τ	$\|e_{h\tau}\|_{L^2(H^1)}$	η_A	η_S	η_T	η_{ST}	η_T/η_S	CPU(s)
1	1	2.0E-01	1.56E+00	4.27E-03	7.32E+00	1.21E-01	7.32E+00	1.65E-02	408.9
1	1	1.0E-01	1.42E+00	4.19E-03	7.47E+00	3.13E-02	7.47E+00	**4.19E-03**	648.2
1	1	5.0E-02	1.40E+00	4.31E-03	7.50E+00	8.93E-03	7.50E+00	**1.19E-03**	1228.7
1	1	2.5E-02	1.40E+00	2.75E-03	7.50E+00	3.39E-03	7.50E+00	**4.51E-04**	2032.6
1	2	2.0E-01	1.40E+00	4.59E-03	7.42E+00	7.21E-03	7.42E+00	**9.72E-04**	732.5
1	2	1.0E-01	1.40E+00	4.00E-03	7.48E+00	4.12E-03	7.48E+00	**5.51E-04**	1269.6
1	2	5.0E-02	1.40E+00	4.73E-03	7.50E+00	4.74E-03	7.50E+00	**6.31E-04**	2329.8
1	2	2.5E-02	1.40E+00	2.52E-03	7.50E+00	2.52E-03	7.50E+00	**3.35E-04**	3584.9
2	1	2.0E-01	5.44E-01	2.60E-04	5.40E-01	1.22E-01	5.53E-01	2.25E-01	1648.9
2	1	1.0E-01	1.84E-01	3.10E-04	5.63E-01	3.12E-02	5.64E-01	5.55E-02	2291.7
2	1	5.0E-02	1.61E-01	3.33E-04	5.68E-01	7.87E-03	5.68E-01	1.38E-02	4162.1
2	1	2.5E-02	1.60E-01	3.08E-04	5.69E-01	1.99E-03	5.69E-01	**3.50E-03**	7406.3
2	2	2.0E-01	1.60E-01	2.94E-04	5.59E-01	5.35E-03	5.59E-01	**9.59E-03**	3960.3
2	2	1.0E-01	1.60E-01	3.35E-04	5.67E-01	7.63E-04	5.67E-01	**1.35E-03**	5508.1
2	2	5.0E-02	1.60E-01	2.81E-04	5.69E-01	2.95E-04	5.69E-01	**5.19E-04**	10267.2
2	2	2.5E-02	1.60E-01	3.29E-04	5.69E-01	3.30E-04	5.69E-01	**5.79E-04**	19839.2
3	1	2.0E-01	5.10E-01	1.92E-05	3.80E-02	1.22E-01	1.27E-01	3.20E+00	5545.3
3	1	1.0E-01	8.85E-02	2.16E-05	4.11E-02	3.12E-02	5.17E-02	7.59E-01	9230.0
3	1	5.0E-02	2.20E-02	1.97E-05	4.19E-02	7.86E-03	4.26E-02	1.88E-01	15655.3
3	1	2.5E-02	1.58E-02	2.07E-05	4.20E-02	1.97E-03	4.20E-02	4.69E-02	25684.9
3	2	2.0E-01	2.10E-02	1.96E-05	4.07E-02	5.35E-03	4.10E-02	1.31E-01	15842.2
3	2	1.0E-01	1.54E-02	1.98E-05	4.17E-02	6.82E-04	4.17E-02	1.64E-02	25593.7
3	2	5.0E-02	1.54E-02	2.22E-05	4.19E-02	8.85E-05	4.19E-02	**2.11E-03**	39928.9
3	2	2.5E-02	1.55E-02	2.00E-05	4.20E-02	2.27E-05	4.20E-02	**5.40E-04**	74548.5
1	1	adapt	1.47E+00	4.06E-03	7.41E+00	7.19E-02	7.41E+00	**9.71E-03**	490.8
1	2	adapt	1.50E+00	3.43E-03	7.07E+00	6.59E-02	7.07E+00	**9.32E-03**	451.3
2	1	adapt	1.60E-01	3.16E-04	5.69E-01	5.56E-03	5.69E-01	**9.77E-03**	4604.2
2	2	adapt	1.60E-01	3.16E-04	5.59E-01	5.35E-03	5.59E-01	**9.57E-03**	3828.8
3	1	adapt	1.55E-02	2.21E-05	4.20E-02	4.12E-04	4.20E-02	**9.80E-03**	54758.5
3	2	adapt	1.54E-02	2.03E-05	4.18E-02	4.04E-04	4.18E-02	**9.66E-03**	28162.8

isotropic

p	q	ω	$\|e_{h\tau}\|_{L^2(H^1)}$	η_A	η_S	η_T	η_{ST}	i_X	CPU(s)
3	2	4.0E-01	1.82E-01	1.97E-03	3.46E-01	1.27E-02	3.46E-01	1.90	1840.5
3	2	1.0E-01	4.63E-02	4.85E-04	8.68E-02	3.61E-03	8.69E-02	1.88	6628.5
3	2	2.5E-02	1.23E-02	1.34E-04	2.22E-02	1.02E-03	2.22E-02	1.81	23750.4

anisotropic

p	q	ω	$\|e_{h\tau}\|_{L^2(H^1)}$	η_A	η_S	η_T	η_{ST}	i_X	CPU(s)
3	2	4.0E-01	1.31E-01	1.13E-03	2.55E-01	1.19E-02	2.56E-01	1.95	2358.1
3	2	1.0E-01	4.08E-02	3.31E-04	6.81E-02	3.55E-03	6.82E-02	1.67	7856.2
3	2	2.5E-02	1.22E-02	1.05E-04	1.83E-02	9.95E-04	1.83E-02	1.50	28603.4

Table 5: Isentropic vortex propagation: the errors $\|e_{h\tau}\|_{L^2(H^1)}$, error estimators η_{A}, η_{S}, η_{T}, η_{ST}, the ratio $\eta_{\mathrm{T}}/\eta_{\mathrm{S}}$, (results with $\eta_{\mathrm{T}}/\eta_{\mathrm{S}} \leq 0.01$ are bolted) and the computational time. For isotropic/anisotropic mesh adaptation, $i_X = \eta_{\mathrm{ST}}/\|e_{h\tau}\|_{L^2(H^1)}$.

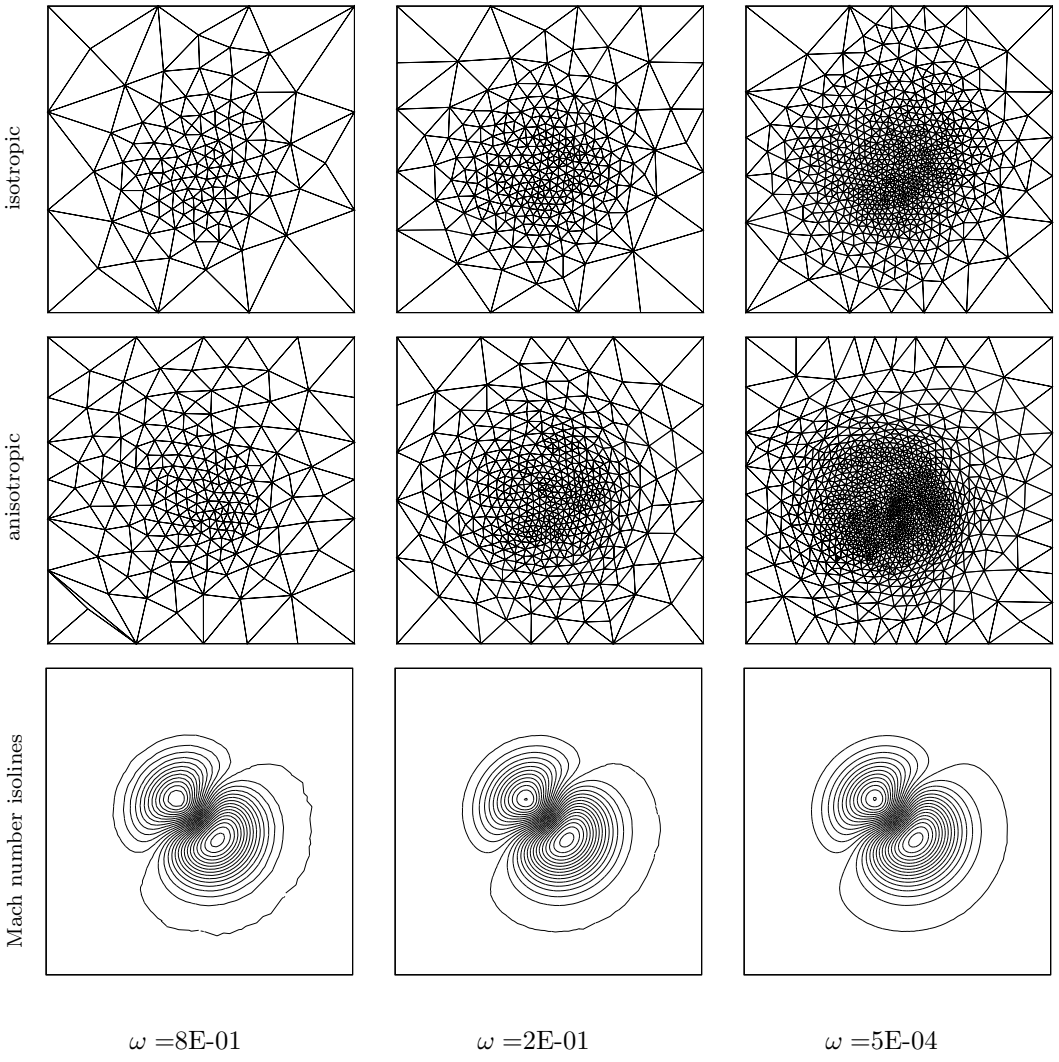

Figure 4: Isentropic vortex: grids generated by the isotropic and the anisotropic mesh adaptation techniques for all tolerances at final time $t = 10$; the corresponding isolines of the Mach number.

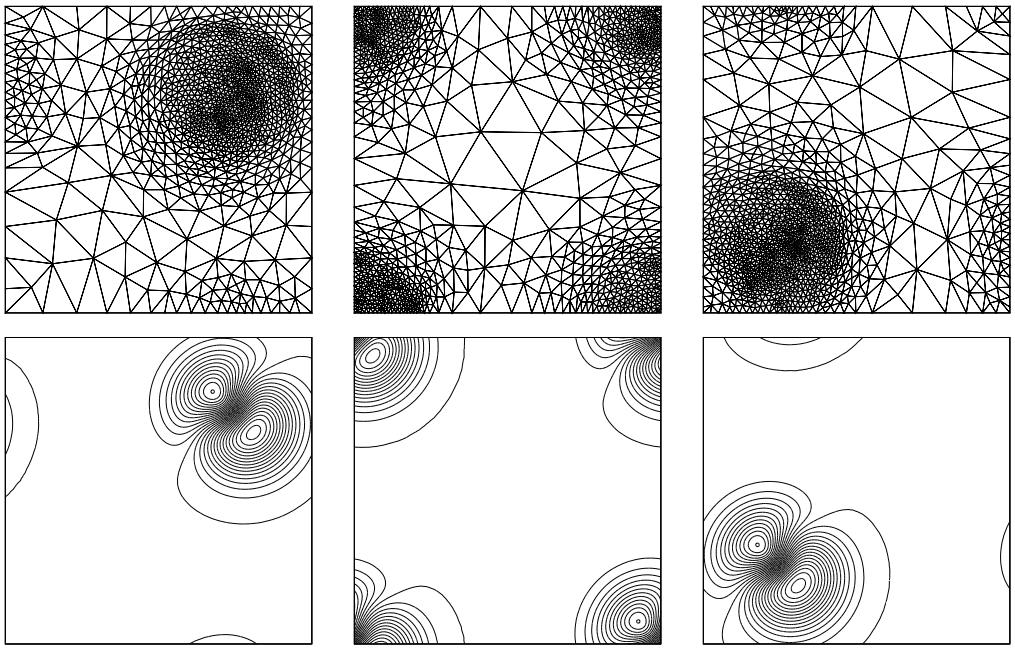

$t = 2.5$ $t = 5.0$ $t = 7.5$

Figure 5: Isentropic vortex

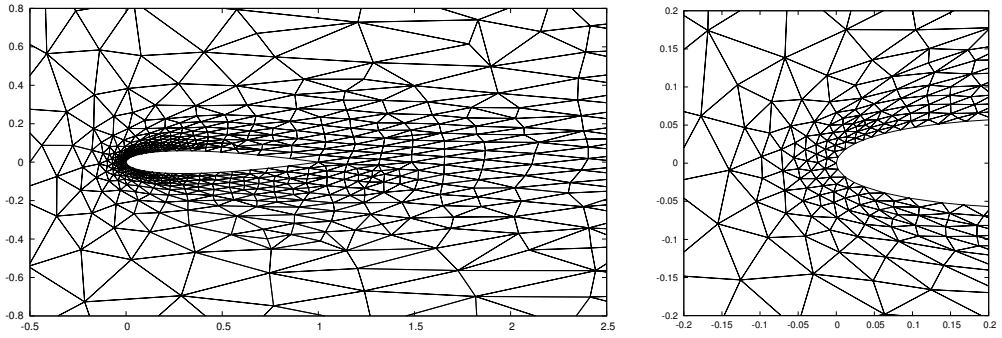

Figure 6: Computational grid for the subsonic flow around NACA0012, details around the profile (left) and its leading edge (right).

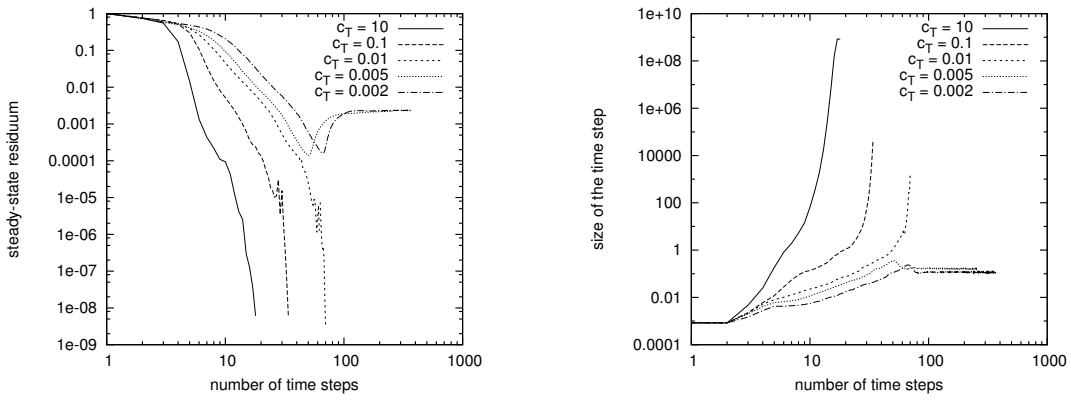

Figure 7: Viscous subsonic flow $c_T = 10$, $c_T = 0.1$ and $c_T = 0.005$, steady-state residuum (left) and the size of τ_k (right) with respect to the number of time steps.

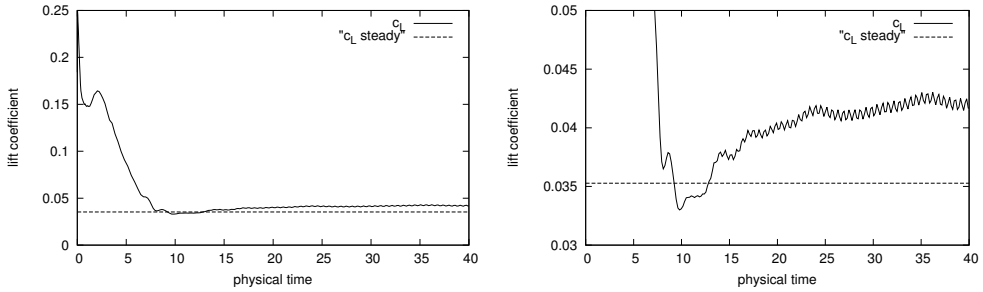

Figure 8: Viscous subsonic flow, time evolution of the lift coefficient c_L with respect the physical time for the setting $c_T = 0.005$ (left) and its detail (right), the value c_L "steady" was obtain with $c_T = 10$ and/or $c_T = 0.1$.

These experiments indicate that an insufficiently accurate resolution with respect to time may lead a different flow regime (steady-flow vs. non-steady). These results are in agreement with [5], where this example was solved by several research groups. They achieved mostly the steady state solution using steady-state solvers or implicit time discretizations (with large time steps). Only a sufficiently accurate (explicit) time discretization (carried out by University of Stuttgart) gave the unsteady flow regime, see [5, Chapter 5].

These observations are in agreement with our results [13] carried out for the three step BDF discretization with respect to time. Moreover, the BDF as well as the time DG discretization techniques required approximately the same computational time (approximately 24 000 s) although the algebraic systems arising from the time DG discretizations are three times larger.

6.3. Numerical simulation of viscous shock-vortex interaction

Similarly as in [59, 60, 61, 13], we consider the viscous interaction of a plane weak shock wave with a single isentropic vortex. During the interaction, acoustic waves are produced, and we investigate the ability of the numerical scheme to capture these waves. The computational domain is $\Omega = (0, 2) \times (0, 2)$ with the periodic extension in the x_2-direction. A stationary plane shock wave is located at $x_1 = 1$. The prescribed pressure jump through the shock is $\mathtt{p}_R - \mathtt{p}_L = 0.4$, where $\mathtt{p}_L$ and $\mathtt{p}_R$ are the pressure values from the left and right of the shock wave, respectively, corresponding to the inlet (left) Mach number $M_L = 1.1588$. The reference density and velocity are

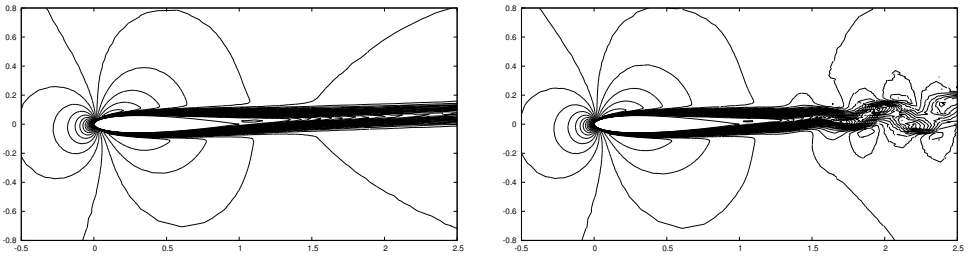

Figure 9: Viscous subsonic flow, isolines of the Mach number for the setting $c_T = 10$ (left) and $c_T = 0.005$ (right).

those of the free uniform flow at infinity. In particular, we define the initial density, x_1-component of velocity and pressure by

$$\rho_L = 1,\ u_L = M_L \gamma^{1/2},\ \mathtt{p}_L = 1, \quad \rho_R = \rho_L K_1,\ u_R = u_L K_1^{-1},\ \mathtt{p}_R = \mathtt{p}_1 K_2,$$

where

$$K_1 = \frac{\gamma+1}{2} \frac{M_L^2}{1 + \frac{\gamma-1}{2} M_L^2}, \quad K_2 = \frac{2}{\gamma+1} \left(\gamma M_L^2 - \frac{\gamma-1}{2} \right).$$

Here, the subscripts $_L$ and $_R$ denote the quantities at $x < 1$ and $x > 1$, respectively, $\gamma = 1.4$ is the Poisson constant. The Reynolds number is 2000. An isolated isentropic vortex centered at $(0.5, 1)$ is added to the basic flow. The angular velocity in the vortex is given by

$$v_\theta = c_1 r \exp(-c_2 r^2), \quad c_1 = u_c / r_c, \quad c_2 = r_c^{-2}/2, \quad r = ((x_1 - 0.5)^2 - (x_2 - 1)^2)^{1/2},$$

where we set $r_c = 0.075$ and $u_c = 0.5$. The computations are stopped at the dimensionless time $T = 0.7$.

We solved this problem with the aid of algorithm from Section 4.6 with setting $c_A := 10^{-2}$, $c_T := 10^{-1}$, $p = 3$ polynomial approximation with respect to space, $q = 2$ polynomial approximation with respect to time and the anisotropic mesh adaptation. We used the tolerance $\omega = 0.02$.

Figure 10 shows the space-time adaptive computations, namely the dependence of the number of degrees of freedom $N_m = 2(p+1)(p+2)(q+1) \# \mathscr{T}_{h,m} = 120 \# \mathscr{T}_{h,m}$ (top left), the size time step τ_m (top right) and the accumulated residual error estimators

$$\eta_{\mathrm{A}}^{\mathrm{acc},m} := \left(\sum_{k=1}^{m} (\eta_{\mathrm{A}}^k)^2 \right)^{1/2}, \qquad \eta_{\mathrm{T}}^{\mathrm{acc},m} := \left(\sum_{k=1}^{m} (\eta_{\mathrm{T}}^k)^2 \right)^{1/2}, \qquad \eta_{\mathrm{ST}}^{\mathrm{acc},m} := \left(\sum_{k=1}^{m} (\eta_{\mathrm{ST}}^k)^2 \right)^{1/2} \tag{71}$$

(bottom left) on $t_m \in [0, T]$. Each node corresponds to one time step. Obviously, $\eta_{\mathrm{A}}^{\mathrm{acc},r} = \eta_{\mathrm{A}}$, $\eta_{\mathrm{T}}^{\mathrm{acc},r} = \eta_{\mathrm{T}}$ and $\eta_{\mathrm{ST}}^{\mathrm{acc},r} = \eta_{\mathrm{ST}}$ since $t_r = T$.

We observe several jumps back with respect to t_m which correspond to re-meshings of the computational grid at several time steps and their repetitions, see step (5) of the adaptive process from Section 4.6. Each re-meshing is usually accompanied by a decrease of the corresponding time step. Moreover, Figure 10 (bottom right) shows the accumulated computational times (CPU) in seconds necessary for the assembling the algebraic systems including the assembling of the flux matrix ("CPU prepare"), CPU for the solution of the corresponding algebraic problems ("CPU solve") and CPU for the evaluation of the residual error estimates ("CPU estim"). We observe that the evaluation of the residual error estimates is not time consuming, it requires less than 3% of the total computational time. On the other hand, the most time consuming is the solution of algebraic systems, hence a more efficient technique should be developed, e.g., the so-called p-multigrid approach seems to be promising.

Finally, Figure 11 shows the used meshes, pressure isolines and the pressure distribution along the horizontal cut at $t = 0$, $t = 0.3$, $t = 0.45$ and $t = 0.6$. We observe a strong anisotropic refinement along the static shock wave which is almost independent on t and a isotropic refinement

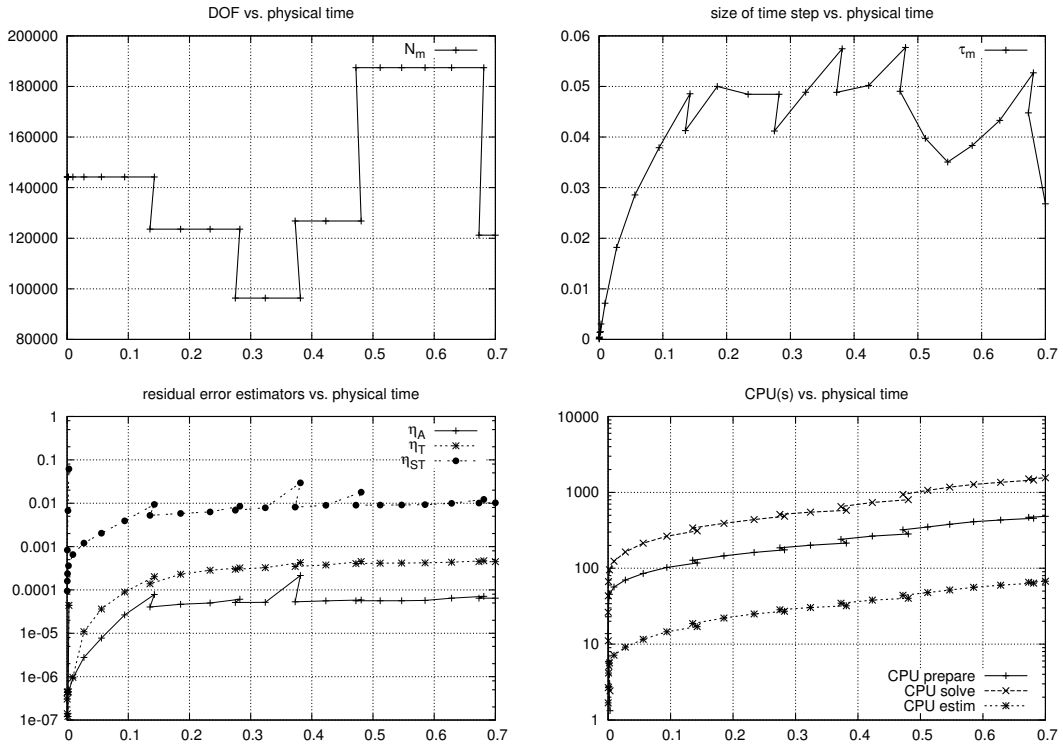

Figure 10: Viscous shock-vortex interaction: space-time adaptive computations, development of the number of degrees of freedom N_m (top left), time step τ_m (top right), the accumulated residual error estimators $\eta_{\mathrm{A}}^{\mathrm{acc},m}$, $\eta_{\mathrm{T}}^{\mathrm{acc},m}$ and $\eta_{\mathrm{ST}}^{\mathrm{acc},m}$, cf. (71) (bottom left) and the computational time (bottom right) with respect $t_m \in [0.0.7]$, each node corresponds to one time step.

around the vortex which moves in the flow direction. The interaction is captured with nonphysical oscillations; let us note the we do not include any stabilization in the numerical scheme. The oscillation-free approximation is the consequence of a high order DG approximation and the anisotropic adaptation.

7. Conclusion

We presented a higher order numerical method for the solution of the non-stationary compressible Navier-Stokes equations, which is based on the space-time discontinuous Galerkin. We developed the residual error estimates technique, which approximates the error measured in the dual norm. This approach is able to identify the several ingredients of the total error, namely its algebraic, spatial and temporal parts. Based on them we defined an adaptive algorithm which

i) solves the corresponding algebraic systems until the algebraic error estimate does not influence the spatial error estimate,

ii) chooses the time step such that the temporal error estimate is controlled by the spatial error estimate,

iii) adapts the mesh in such a way that the space-time error estimate is under a given tolerance.

Several numerical experiments confirmed these items and demonstrated the ability of the presented method.

The main drawback of the presented approach is that we have no information about the real size of the error. The development of such error estimator is the subject of further research. The most promising approach seems to us the goal-oriented a posteriori error estimation, cf. [31, 32]. Another challenge is a use of these residual error estimates for an anisotropic *hp*-adaptive method.

Appendix A. Choice of $\|\cdot\|_X$

Here, our aim is to give a (partial) theoretical justification for the choice of $\|\cdot\|_X$ in (53). For simplicity, we consider a linear problem $u' - \Delta u = f$ on $\Omega \times (0,T)$ with homogeneous boundary condition and initial condition u_0. We introduce the following *weak formulation*: let $u \in L^2(0,T,H_0^1(\Omega))$ be such that

$$\int_0^T (-u, v') + (\nabla u, \nabla v)\,\mathrm{d}t = \int_0^T (f,v)\,\mathrm{d}t + (u_0, v(0)) \quad \forall v \in X, \tag{A.1}$$

where the space X is defined as

$$X = \{v \in L^2(0,T,H_0^1(\Omega)) : v' \in L^2(0,T,H^{-1}), v(T) = 0\}, \tag{A.2}$$

see, e.g., [29]. Let us assume the discrete solution $u_{h\tau}$ obtained by conforming method, i.e. $u_{h\tau}$ belongs to a subspace of $L^2(0,T,H_0^1(\Omega))$ and satisfy relation (A.1) for all $v_h \in X_h \subset X$. Then, according to (37), the residual measure of the error $e = u - u_{h\tau}$ can be expressed as

$$\mathcal{R} = \sup_{0\neq v\in X} \frac{\int_0^T (f,v) + (u_{h\tau}, v') - (\nabla u_{h\tau}, \nabla v)\,\mathrm{d}t + (u_0, v(0))}{\|v\|_X} = \sup_{0\neq v\in X} \frac{\int_0^T (-e, v') + (\nabla e, \nabla v)\,\mathrm{d}t}{\|v\|_X}. \tag{A.3}$$

Our aim is to choose the norm $\|\cdot\|_X$ in such a way that the term $\mathcal{R}$ is equivalent to the $L^2(0,T,H_0^1(\Omega))$-norm of the error. We present the following results.

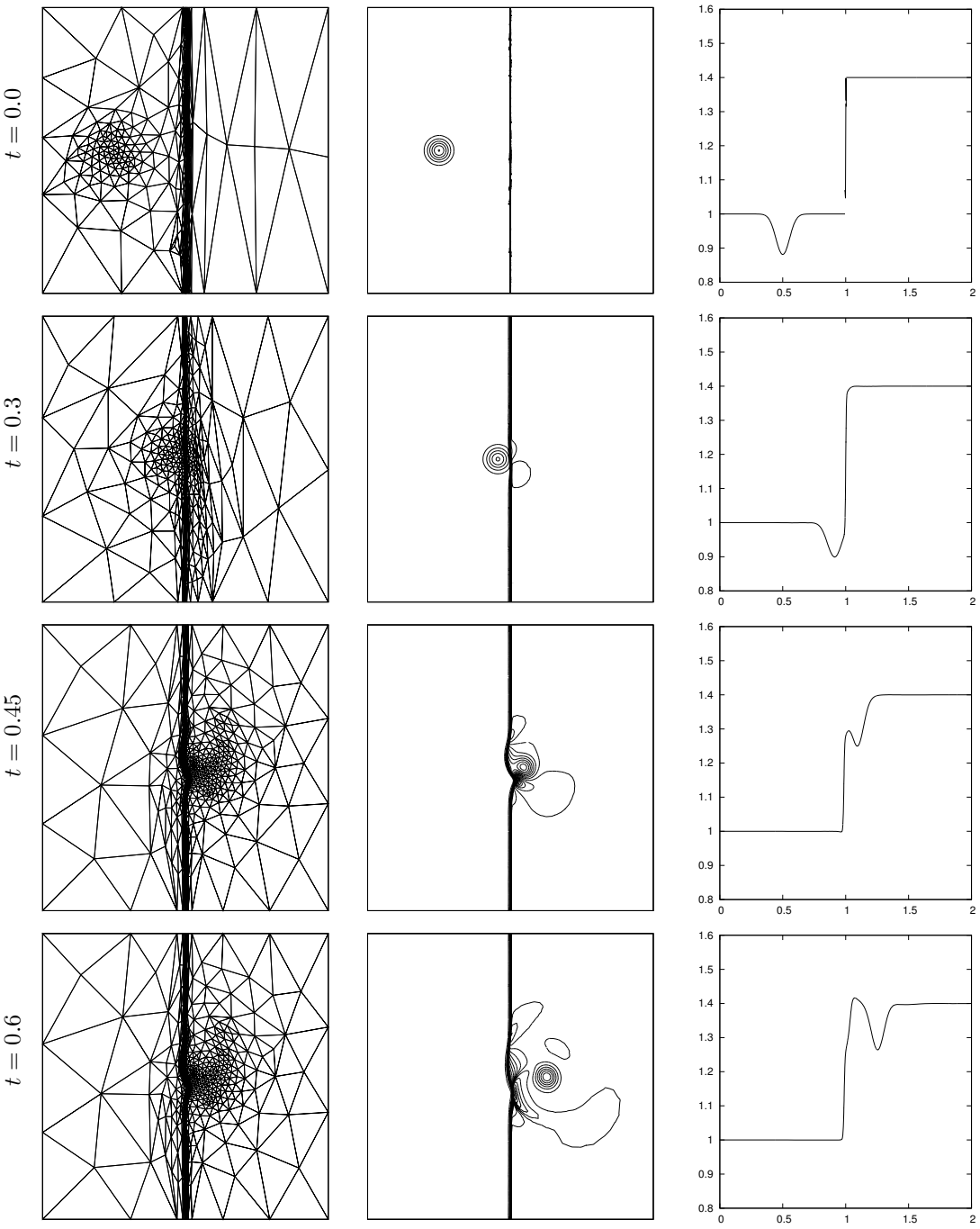

Figure 11: Viscous shock-vortex interaction: meshes, pressure isolines and the pressure distribution along the horizontal cut at $t = 0$, $t = 0.3$, $t = 0.45$ and $t = 0.6$.

Lemma Appendix A.1. *Let* $\|v\|_X := \|v\|_{L^2(0,T,H_0^1(\Omega))} + \|v'\|_{L^2(0,T,H^{-1}(\Omega))}$, *then*

$$\mathcal{R} \le \|e\|_{L^2(0,T,H_0^1(\Omega))} \le 3\mathcal{R}. \tag{A.4}$$

Proof. Obviously, $\mathcal{R} \le \|e\|_{L^2(0,T,H_0^1(\Omega))}$, since the Hölder inequality gives

$$\int_0^T (-e, v') + (\nabla e, \nabla v)\,\mathrm{d}t \le \|e\|_{L^2(0,T,H_0^1(\Omega))}\|v'\|_{L^2(0,T,H^{-1}(\Omega))} + \|e\|_{L^2(0,T,H_0^1(\Omega))}\|v\|_{L^2(0,T,H_0^1(\Omega))} = \|e\|_{L^2(0,T,H_0^1(\Omega))}\|v\|_X.$$

In order to prove the opposite inequality $\|e\|_{L^2(0,T,H_0^1(\Omega))} \le 3\mathcal{R}$, we consider the dual problem: find solution $z \in X$ such that

$$\int_0^T (-z', w) + (\nabla z, \nabla w)\,\mathrm{d}t = \int_0^T (\nabla e, \nabla w)\,\mathrm{d}t \quad \forall w \in L^2(0,T,H_0^1(\Omega)). \tag{A.5}$$

Let z be the solution of (A.5). We show that

$$\|z\|_{L^2(0,T,H_0^1(\Omega))} + \|z'\|_{L^2(0,T,H^{-1}(\Omega))} \le 3\|e\|_{L^2(0,T,H_0^1(\Omega))}. \tag{A.6}$$

Putting $w := z$ in (A.5), we get

$$-\frac{1}{2}\|z(T)\|^2_{L^2(\Omega)} + \frac{1}{2}\|z(0)\|^2_{L^2(\Omega)} + \|z\|^2_{L^2(0,T,H_0^1(\Omega))} = \int_0^T (\nabla e, \nabla z)\,\mathrm{d}t \le \|e\|_{L^2(0,T,H_0^1(\Omega))}\|z\|_{L^2(0,T,H_0^1(\Omega))},$$

hence we have $\|z\|_{L^2(0,T,H_0^1(\Omega))} \le \|e\|_{L^2(0,T,H_0^1(\Omega))}$. Moreover, the definitions of the $L^2(0,T,H^{-1}(\Omega))$- and $L^2(0,T,H_0^1(\Omega))$- norms imply

$$\begin{aligned}
\|z'\|_{L^2(0,T,H^{-1}(\Omega))} &= \sup_{0\neq w\in L^2(0,T,H_0^1(\Omega))} \frac{\int_0^T (z', w)}{\|w\|_{L^2(0,T,H_0^1(\Omega))}} \\
&\le \sup_{0\neq w\in L^2(0,T,H_0^1(\Omega))} \frac{\int_0^T (z', w) - (\nabla z, \nabla w)\,\mathrm{d}t}{\|w\|_{L^2(0,T,H_0^1(\Omega))}} + \sup_{0\neq w\in L^2(0,T,H_0^1(\Omega))} \frac{\int_0^T (\nabla z, \nabla w)\,\mathrm{d}t}{\|w\|_{L^2(0,T,H_0^1(\Omega))}} \\
&= \sup_{0\neq w\in L^2(0,T,H_0^1(\Omega))} \frac{-\int_0^T (\nabla e, \nabla w)\,\mathrm{d}t}{\|w\|_{L^2(0,T,H_0^1(\Omega))}} + \sup_{0\neq w\in L^2(0,T,H_0^1(\Omega))} \frac{\int_0^T (\nabla z, \nabla w)\,\mathrm{d}t}{\|w\|_{L^2(0,T,H_0^1(\Omega))}} \\
&= \|e\|_{L^2(0,T,H_0^1(\Omega))} + \|z\|_{L^2(0,T,H_0^1(\Omega))}.
\end{aligned}$$

From this inequality it follows that $\|z'\|_{L^2(0,T,H^{-1}(\Omega))} \le 2\|e\|_{L^2(0,T,H_0^1(\Omega))}$ and therefore (A.6) is valid. Finally, from (A.6) and (A.5) with $w := e$, we get

$$\|e\|_{L^2(0,T,H_0^1(\Omega))} \le \frac{3\|e\|^2_{L^2(0,T,H_0^1(\Omega))}}{\|z\|_{L^2(0,T,H_0^1(\Omega))} + \|z'\|_{L^2(0,T,H^{-1}(\Omega))}} = \frac{3\int_0^T (-e, z') + (\nabla e, \nabla z)\,\mathrm{d}t}{\|z\|_{L^2(0,T,H_0^1(\Omega))} + \|z'\|_{L^2(0,T,H^{-1}(\Omega))}} \le 3\mathcal{R}.$$

□

Lemma Appendix A.1 gives the equivalence between the residual measure $\mathcal{R}$ and the norm $L^2(0,T,H_0^1(\Omega))$ defined therein for a conforming approximation. However, the norm defined by (53) and the norm $\|\cdot\|_X$ defined by this Lemma are not the same. Although both of the norms contain a term consisting of a norm of the time derivative, the latter involves the H^{-1}-norm with respect to the space variables, whereas the norm defined in (53) contains the H^1-norm.

[1] F. Bassi, S. Rebay, A high-order accurate discontinuous finite element method for the numerical solution of the compressible Navier–Stokes equations, J. Comput. Phys. 131 (1997) 267–279.

[2] F. Bassi, S. Rebay, A high order discontinuous Galerkin method for compressible turbulent flow, in: B. Cockburn, G. E. Karniadakis, C.-W. Shu (Eds.), Discontinuous Galerkin Method: Theory, Computations and Applications, Lecture Notes in Computational Science and Engineering 11, Springer-Verlag, 2000, pp. 113–123.

[3] I. Lomtev, C. B. Quillen, G. E. Karniadakis, Spectral/*hp* methods for viscous compressible flows on unstructured 2d meshes, J. Comput. Phys. 144 (2) (1998) 325–357.

[4] C. E. Baumann, J. T. Oden, A discontinuous *hp* finite element method for the Euler and Navier-Stokes equations, Int. J. Numer. Methods Fluids 31 (1) (1999) 79–95.

[5] N. Kroll, H. Bieler, H. Deconinck, V. Couallier, H. van der Ven, K. Sorensen (Eds.), ADIGMA - A European Initiative on the Development of Adaptive Higher-Order Variational Methods for Aerospace Applications, Vol. 113 of Notes on Numerical Fluid Mechanics and Multidisciplinary Design, Springer Verlag, 2010.

[6] F. Vilar, P. Maire, R. Abgrall, Cell-centered discontinuous Galerkin discretizations for two-dimensional scalar conservation laws on unstructured grids and for one-dimensional lagrangian hydrodynamics, Computers and Fluids 46 (1) (2011) 498–504.

[7] F. Hindenlang, G. J. Gassner, C. Altmann, A. Beck, M. Staudenmaier, C.-D. Munz, Explicit discontinuous Galerkin methods for unsteady problems, Comput. Fluids 61 (2012) 86–93.

[8] A. Ern, I. Mozolevski, Discontinuous Galerkin method for two-component liquid-gas porous media flows, Computational Geosciences 16 (3) (2012) 677–690.

[9] F. Bassi, L. Botti, A. Colombo, S. Rebay, Agglomeration based discontinuous Galerkin discretization of the Euler and Navier-Stokes equations, Computers and Fluids 61 (2012) 77–85.

[10] S. Giani, P. Houston, Anisotropic *hp*-adaptive discontinuous Galerkin finite element methods for compressible fluid flows, Int. J. Numer. Anal. Model. 9 (4) (2012) 928–949.

[11] J. Česenek, M. Feistauer, J. Horáček, V. Kučera, J. Prokopová, Simulation of compressible viscous flow in time-dependent domains, Appl. Math. Comput. 219 (13) (2011) 7139–7150.

[12] V. Dolejší, M. Holík, J. Hozman, Efficient solution strategy for the semi-implicit discontinuous Galerkin discretization of the Navier-Stokes equations, J. Comput. Phys. 230 (2011) 4176–4200.

[13] V. Dolejší, A design of residual error estimates for a high order BDF-DGFE method applied to compressible flows, Int. J. Numer. Meth. Fluids 73 (6) (2013) 523–559.

[14] M. Vlasák, V. Dolejší, J. Hájek, A priori error estimates of an extrapolated space-time discontinuous Galerkin method for nonlinear convection-diffusion problems, Numer. Methods Partial Differ. Equations 26 (2011) 1456–1482.

[15] J. J. W. van der Vegt, H. van der Ven, Space-time discontinuous Galerkin finite element method with dynamic grid motion for inviscid compressible flows. I: General formulation, J. Comput. Phys. 182 (2) (2002) 546–585.

[16] H. van der Ven, J. J. W. van der Vegt, Space-time discontinuous Galerkin finite element method with dynamic grid motion for inviscid compressible flows II. efficient flux quadrature, Comput. Methods Appl. Mech. Engrg. 191 (2002) 4747–4780.

[17] C. M. Klaij, J. van der Vegt, H. V. der Ven, Pseudo-time stepping for space-time discontinuous Galerkin discretizations of the compressible Navier-Stokes equations, J. Comput. Phys. 219 (2) (2006) 622–643.

[18] C. M. Klaij, J. van der Vegt, H. V. der Ven, Space-time discontinuous Galerkin method for the compressible Navier-Stokes equations, J. Comput. Phys. 217 (2) (2006) 589–611.

[19] C. M. Klaij, M. H. van Raalte, H. van der Ven, H. J. W. van der Vegt, h-multigrid for space-time discontinuous Galerkin discretizations of the compressible Navier-Stokes equations, J. Comput. Phys. 227 (2007) 1024–1045.

[20] G. Gassner, F. Lörcher, C.-D. Munz, A discontinuous Galerkin scheme based on a spacetime expansion. I. Inviscid compressible flow in one space dimension, J. Sci. Comput. 32 (2) (2007) 175–199.

[21] G. Gassner, F. Lörcher, C.-D. Munz, A discontinuous Galerkin scheme based on a spacetime expansion. II. viscous flow equations in multi dimensions, J. Sci. Comput. 34 (3) (2008) 260–286.

[22] J. Česenek, M. Feistauer, Theory of the space-time discontinuous Galerkin method for nonstationary parabolic problems with nonlinear convection and diffusion, SIAM J. Numer. Anal. 30 (2012) 1181–1206.

[23] M. Feistauer, V. Kučera, K. Najzar, J. Prokopová, Analysis of space-time discontinuous Galerkin method for nonlinear convection-diffusion problems, Numer. Math. 117 (2011) 251–288.

[24] G. Akrivis, C. Makridakis, R. H. Nochetto, A posteriori error estimates for the Crank-Nicolson method for parabolic equations, Math. Comp. 75 (254) (2006) 511–531.

[25] P. Ladevèze, N. Moës, A new a posteriori error estimation for nonlinear time-dependent finite element analysis, Comput. Methods Appl. Mech. Engrg. 157 (1-2) (1998) 45–68.

[26] R. H. Nochetto, A. Schmidt, C. Verdi, A posteriori error estimation and adaptivity for degenerate parabolic problems, Math. Comput. 69 (229) (2000) 1–24.

[27] R. Verfürth, A posteriori error estimates for nonlinear problems: $L^r(0,T;W^{1,\rho}(\Omega))$-error estimates for finite element discretizations of parabolic equations, Numer. Meth. Part. Diff. Eqs 14 (1998) 487–518.

[28] R. Verfürth, A posteriori error estimates for nonlinear problems: $L^r(0,T;L^\rho(\Omega))$-error estimates for finite element discretizations of parabolic equations, Math. Comput. 67 (224) (1998) 1335–1360.

[29] V. Dolejší, A. Ern, M. Vohralík, A framework for robust a posteriori error control in unsteady nonlinear advection-diffusion problems, SIAM J. Numer. Anal. 51 (2) (2013) 773–793.

[30] R. Hartmann, P. Houston, Symmetric interior penalty DG methods for the compressible Navier-Stokes equations II: Goal-oriented a posteriori error estimation., Int. J. Numer. Anal. Model. 3 (2006) 141–162.

[31] R. Becker, R. Rannacher, An optimal control approach to a-posteriori error estimation in finite element methods, Acta Numerica 10 (2001) 1–102.

[32] M. Giles, E. Süli, Adjoint methods for PDEs: a posteriori error analysis and postprocessing by duality, Acta Numerica 11 (2002) 145–236.

[33] T. J. Barth, Space-time error representation and estimation in Navier-Stokes calculations, in: Complex Effects in Large Eddy Simulations, Vol. 56 of Lecture Notes in Computational Science and Engineering, Springer-Verlag, 2007, pp. 29–48.

[34] K. J. Fidkowski, Y. Luo, Output-based space-time mesh adaptation for the compressible Navier-Stokes equations, J. Comput. Phys. 230 (14) (2011) 5753–5773.

[35] V. Dolejší, Semi-implicit interior penalty discontinuous Galerkin methods for viscous compressible flows, Commun. Comput. Phys. 4 (2) (2008) 231–274.

[36] M. Feistauer, J. Felcman, I. Straškraba, Mathematical and Computational Methods for Compressible Flow, Oxford University Press, Oxford, 2003.

[37] M. Feistauer, V. Kučera, On a robust discontinuous Galerkin technique for the solution of compressible flow, J. Comput. Phys. 224 (1) (2007) 208–221.

[38] A. Kufner, O. John, S. F. k, Function Spaces, Academia, Prague, 1977.

[39] J. Nečas, Les Méthodes Directes en Thèorie des Equations Elliptiques, Academia, Prague, 1967.

[40] V. Thomée, Galerkin finite element methods for parabolic problems. 2nd revised and expanded ed., Berlin, Springer, 2006.

[41] D. Schötzau, C. Schwab, An *hp* a priori error analysis of the discontinuous Galerkin time-stepping for initial value problems, Calcolo 37 (2000) 207–232.

[42] V. Dolejší, Analysis and application of IIPG method to quasilinear nonstationary convection-diffusion problems, J. Comp. Appl. Math. 222 (2008) 251–273.

[43] V. Dolejší, M. Feistauer, Semi-implicit discontinuous Galerkin finite element method for the numerical solution of inviscid compressible flow, J. Comput. Phys. 198 (2) (2004) 727–746.

[44] P. Deuflhard, Newton Methods for Nonlinear Problems, Vol. 35 of Springer Series in Computational Mathematics, Springer, 2004.

[45] Y. Saad, M. H. Schultz, GMRES: A generalized minimal residual algorithm for solving non-symmetric linear systems, SIAM J. Sci. Stat. Comput. 7 (1986) 856–869.

[46] E. Hairer, S. P. Norsett, G. Wanner, Solving ordinary differential equations I, Nonstiff problems, no. 8 in Springer Series in Computational Mathematics, Springer Verlag, 2000.

[47] E. Hairer, G. Wanner, Solving ordinary differential equations II, Stiff and differential-algebraic problems, Springer Verlag, 2002.

[48] L. E. Alaoui, A. Ern, M. Vohralík, Guaranteed and robust a posteriori error estimates and balancing discretization and linearization errors for monotone nonlinear problems, Comput. Methods Appl. Mech. Engrg 200 (2011) 2782–2795.

[49] E. Burman, A. Ern, Discontinuous Galerkin approximation with discrete variational principle for the nonlinear Laplacian, Comptes Rendus Mathematique 346 (17-18) (2008) 1013–1016.

[50] A. Chaillou, M. Suri, A posteriori estimation of the linearization error for strongly monotone nonlinear operators, J. Comput. Appl. Math. 205 (1) (2007) 72–87.

[51] V. Dolejší, *hp*-DGFEM for nonlinear convection-diffusion problems, Math. Comput. Simul. 87 (2013) 87–118.

[52] V. Dolejší, P. Kůs, Adaptive backward difference formula – discontinuous Galerkin finite element method for the solution of conservation laws, Int. J. Numer. Methods Eng. 73 (12) (2008) 1739–1766.

[53] V. Dolejší, Anisotropic mesh adaptation for finite volume and finite element methods on triangular meshes, Comput. Vis. Sci. 1 (3) (1998) 165–178.

[54] V. Dolejší, ANGENER – software package, Charles University Prague, Faculty of Mathematics and Physics, www.karlin.mff.cuni.cz/ dolejsi/angen.html (2000).

[55] V. Dolejší, Anisotropic *hp*-adaptive discontinuous Galerkin method for the numerical solution of time dependent PDEs, Applied Mathematics and ComputationArticle in Press. doi:10.1016/j.amc.2014.12.099.

[56] I. Babuška, M. Suri, The *p*- and *hp*- versions of the finite element method. An overview, Comput. Methods Appl. Mech. Eng. 80 (1990) 5–26.

[57] V. Dolejší, M. Feistauer, V. Kučera, V. Sobotíková, An optimal $L^\infty(L^2)$-error estimate of the discontinuous Galerkin method for a nonlinear nonstationary convection-diffusion problem, IMA J. Numer. Anal. 28 (3) (2008) 496–521.

[58] C. Shu, Essentially non-oscillatory and weighted essentially non-oscillatory schemes for hyperbolic conservation laws, in: A. Q. et al (Ed.), Advanced numerical approximation of nonlinear hyperbolic equations, Lect. Notes Math. 1697, Berlin: Springer, 1998, pp. 325–432.

[59] V. Daru, C. Tenaud, High order one-step monotonicity-preserving schemes for unsteady compressible flow calculations, J. Comput. Phys. 193 (2) (2004) 563–594.

[60] J. Fürst, Modélisation numérique d'écoulements transsoniques avec des schémas TVD et ENO, Ph.D. thesis, Universite Mediterranee, Marseille and Czech Technical University Prague (2001).

[61] C. Tenaud, E. Garnier, P. Sagaut, Evaluation of some high-order shock capturing schemes for direct numerical simulation of unsteady two-dimensional free flows, Int. J. Numer. Meth. Fluids 126 (2000) 202–228.